1-1-1963

Deuterium isotope rate effects in the spontaneous and magnesium-ion-catalyzed decarboxylation of oxalacetic acid.

Stanislava N. Lipovac
University of Windsor

DEUTERIUM ISOTOPE RATE EFFECTS IN THE SPONTANEOUS AND MAGNESIUM-ION-CATALYZED DECARBOXYLATION OF OXALACETIC ACID

A THESIS

Submitted to the Faculty of Graduate Studies,

Assumption University of Windsor,

in Partial Fulfillment of the Requirements

for the Degree of Master of Science.

by

Stanislava N. Lipovac.

Faculty of Graduate Studies,

Assumption University of Windsor.

1963

AB G2523

Approved by: G.W. Kosuchi c.s.s

Roger J. Thibert

Abx Smyth

ABSTRACT

Spectrophotometric studies of the spontaneous and magnesium-ion-catalyzed decarboxylation of oxalacetic acid in Tris-acetate buffer systems in H_2O and D_2O have been carried out over a range of pH and pD.

The mechanism of the catalysis and the inhibition of the decarboxylation of oxalacetic acid are related to the nature of magnesium chelate compound formed under different conditions.

A C K N O W L E D G M E N T

The author wishes to express his sincere gratitude to Rev. George W. Kosicki, C.S.B., Ph.D., Assistant Professor in Chemistry, for his valuable guidance, permanent interest and help during the course of this investigation.

It is a pleasure to thank Dr. Hans H. G. Jellinek, Head of Chemistry Department, for his interest in connection with this work.

The constructive criticisms offered, particularly by Dr. Roger J. Thibert, as well as by Dr. Alex Gnyp and Dr. Kenneth G. Rutherford, and the mathematical assistance of Mr. P. A. Kelly are all gratefully acknowledged.

The author would like to thank the Faculty of Natural Sciences and Mathematics, University of Belgrad, for the opportunity to work abroad and the National Research Council of Canada who made it financially possible.

TABLE OF CONTENTS

Abstract i

Acknowledgment ii

List of Tables iv

List of Figures v

I. INTRODUCTION 1

II. EXPERIMENTAL 15

A. Methods 15

B. Results 15

III. DISCUSSION 40

IV. SUMMARY 47

REFERENCES 48

APPENDIX I. 50

APPENDIX II. 61

Author's Vita 64

LIST OF TABLES

		Page
Table I	Relative Rates of Decomposition of Keto Acids and their Anions in H_2O.	2
Table II	Arrhenius Parameters for Oxalacetic Acid.	3
Table III	The Effect of Temperature on the Decomposition of Oxalacetic Acid.	4
Table IV	Kinetic Constants for the Spontaneous Decarboxylation of Oxalacetic Acid Measured by CO_2 Evolution.	5
Table V	Cupric and Zinc Ion Catalysis in the Decarboxylation of Oxalacetic Acid at 37.0°C.	8
Table VI	Rate Constants and Thermodynamic Association Constants for the Rare Earth Ions and Oxalacetic Acid at 25°C. and Ionic Strength 0.22.	10
Table VII	Rate Coefficients k_cK for Oxalacetic Acid and Transition Metal Ions at 37°C.	10
Table VIII	Keto-Enol Equilibria for Metal Oxalacetate.	11
Table IX	Rate Constants for Chelate Compounds M-OAA at 36.9°C. and Ionic Strength 0.1.	12
Table X	Observed First Order Rate Constants for the Mg++ Catalyzed Decarboxylation of Oxalacetic Acid in H_2O.	31
Table XI	Observed First Order Rate Constants for the Mg++ Catalyzed Decarboxylation of Oxalacetic Acid in D_2O.	32
Table XII	Keto Enol Equilibrium for Magnesium-Oxalacetate Complex.	35

LIST OF FIGURES

		Page
Fig. 1	The Effects of 14 Different Metal Ions on the Rate of Decarboxylation of Oxalacetic Acid at 30°C and pH-5.	7
Fig. 2	The Relative Rates of the Enzymatic Decarboxylation of Oxalacetic Acid in H_2O and in D_2O.	13
Fig. 3	Spontaneous Decarboxylation of Oxalacetic Acid as a Function of pH (pD).	17
Fig. 4	The Spectra of the Magnesium Chelate as a Function of Magnesium Ion Concentration.	19
Fig. 5a,b	The Observed First Order Rate Constant of Decarboxylation of Oxalacetic Acid as a Function of pH and Magnesium Ion Concentration.	22 23
Fig. 6a,b	The Observed First Order Rate Constant of Decarboxylation as a Function of pD and Magnesium Ion Concentration.	25 26
Fig. 7	Absorbance at 280 mμ of the Magnesium Chelate as a Function of pH and pD.	33
Fig. 8	Scott's Plot for the Over-all Association Constant for the Magnesium Chelate.	36
Fig. 9	The Formation of Magnesium Chelate.	38
Fig. 10	Change of the Absorbance with the Time for the Magnesium-Ion-Catalyzed Decarboxylation of Oxalacetic Acid at pH-8. (Appendix I)	58
Fig. 11	First Order Plot for the Magnesium-Ion-Catalyzed Decarboxylation of Oxalacetic Acid at pH-8. (Appendix I).	59

I. INTRODUCTION

The decomposition of oxalacetic acid in aqueous solutions into pyruvic acid and carbon dioxide is an example of the ketonic decomposition exhibited by β-keto acids in general.

$$HO_2C - CO - CH_2 - CO_2H \longrightarrow HO_2C - CO - CH_3 + CO_2 \qquad (1)$$

It has been shown that oxalacetic acid decarboxylates spontaneously (1, 2, 3) and catalytically by the action of aromatic amines (4), a great number of polyvalent cations (1, 5 - 16) and enzymes (17).

The kinetics of the spontaneous decarboxylation of oxalacetic acid in aqueous solution have been studied over a range of temperature and at varying degrees of dissociation (6, 9, 11). Steinberger and Westheimer (18, 19) have proposed that the keto form of the acid decarboxylates by measuring the decarboxylation of α,α-dimethyl substituted oxalacetic acid in which only the keto form can exist. Pedersen (9) studied decarboxylation of oxalacetic acid itself in a solution of potassium and hydrogen chloride and also in acetate buffer at 37°C by observing the pressure of CO_2 evolved above the solution. He proposed that oxalacetic acid in solution of constant ionic strength was present in the form of undissociated acid (OAA) and partly as univalent ion (OAA^-) and divalent ion ($OAA^=$). The kinetic expression has been written in the form:

$$-\frac{dx}{dt} = k_o(OAA) + k_1(OAA^-) + k_2(OAA^=)$$

$$= [k_o + (k_1 - k_o)\cdot\alpha_1 + (k_2 - k_o)\alpha_2\ ]\cdot X \qquad (2)$$

where k_o, k_1, k_2 are rate constants for the spontaneous decarboxylation of the species OAA, OAA^-, $OAA^=$, while α_1 and α_2 are degrees of dissociation

into the ions OAA^- and $OAA^=$ respectively. Experimental measurements showed that the reaction followed the first order kinetics. Pedersen showed that the univalent ion (OAA^-) decomposes 44 times as fast as the undissociated acid.

In Table I a comparison of the relative rates of decarboxylation is given for a number of β-keto acids and their ions.

TABLE I

Relative Rates of Decomposition of Keto Acids and their Anions in H_2O (20)

Acid	Relative Rate		Temperature °C.	Reference
	acid	anion		
Acetoacetic	53	1	37	21
α,α-Dimethylacetoacetic	180	1	18	22
Camphor-3-carboxylic	34	1	98	23
Dihydroxymaleic	1	40	20	24
Acetondicarboxylic	1	2.5	50	24,25
Malonic	10	1	90	26
Oxalacetic	1	44	37	9
Phenylmalonic	1	3	37	27
Dibromomalonic	1	1	37	27

Temperature effects and Arrhenius parameters have been studied by Gelles (11) for the first order decomposition of oxalacetic acid and of its univalent anion.

Arrhenius activation energies and A factors derived from experimental data are given in Table II. The activation energies for the acid and its anion are accurate within $\pm$ 500 and $\pm$ 300 cal/mol, respectively.

TABLE II

Arrhenius Parameters for Oxalacetic Acid

Arrhenius Parameters	Acid	Anion
E (K cal/mol)	25.8	23.1
10^{-13} A(sec^{-1})	0.85	0.48

The data gives further evidence that the monoion of oxalacetic acid is the more active species in decarboxylation.

The effect of temperature on decomposition of oxalacetic acid studied by Nossal (6) is illustrated in Table III.

TABLE III

The Effect of Temperature on the

Decomposition of Oxalacetic Acid

Total volume, 3 ml. Experimental Period 60 mins. at 28°C.

30 mins. at 38°C.

pH	Total CO_2 outputs ($\mu\ell$)		
	at 28°C.	at 38°C.	Theoretical CO_2
6.5	48	92	390
5.0	65	130	390
3.5	94	167	390

Measurements were done with a Warburg apparatus. It can be seen that the increases in evolution of CO_2 as the pH is lowered from 6.5 to 3.5 are of the same order for both temperatures. The same author has investigated the influence of various buffers on the decomposition of oxalacetic acid by measuring total output of CO_2.

Experimental data related to spontaneous decarboxylation of oxalacetic acid under various conditions are summarized in Table IV.

TABLE IV

Kinetic Constants for the Spontaneous Decarboxylation of Oxalacetic Acid Measured by CO_2 Evolution

10^3 k min^{-1}			t°C	pH	Conditions	Ref.
monoion	over-all observed	molecule				
6.53		0.147	37°		0.050 M (HCl+KCl); I 0.05	9
6.56		0.148	37°		0.100 M (HCl+KCl); I 0.10	9
6.57		0.153	37°		0.200 M (HCl+KCl); I 0.20	9
3.40		0.064	25°		0.100 M (HCl+KCl); I 0.1	11
6.67		0.134	30°		0.100 M (HCl+KCl); I 0.1	11
15.4		0.345	37°		0.100 M (HCl+KCl); I 0.1	11
	7.00		37°		0.05 M KCl	13
	2.2		37°	1.02	HCl or $HClO_4$; I = 0.7	13
	1.9		37°	1.02	HCl or $HClO_4$; I = 1.3	13
	0.69		25°		HCl or $HClO_4$; I = 0.22	13
	⁂ 3.2(1.4)		25°	5	0.18 M acetate buffer	2
	⁂ 2.5		30°	6		3
	⁂ 6.0		30°	5	0.1 M acetate buffer	5

Legene: The asterisks ⁂ refer to conditions comparable to data in Fig. 3 (Experimental Part).

The metal-ion-catalyzed decomposition of oxalacetic acid to pyruvic acid and carbon dioxide involves the interaction of metal ions with oxalacetate.

The kinetics of the catalyzed decarboxylation of oxalacetic acid have been studied manometrically and spectrophotometrically.

H. A. Krebs (1) was the first to point out that the enzymatic decarboxylation of oxalacetic acid is promoted by polyvalent ions and that the reaction can be catalyzed by these ions even in the absence of enzyme.

A. Kornberg, S. Ochoa and A. Mehler (10) indicated that aluminium ions form complexes with oxalsuccinic, oxalacetic and acetoacetic acid. Such complexes formed with oxalosuccinic and oxalacetic acid are unstable and decarboxylate at a rate faster than their spontaneous decarboxylation. By contrast, neither the enxymatic (28) nor the nonenzymatic decarboxylations of acetoacetic acid are affected by this ion. These authors showed that Mg^{++} and Mn^{++} also form complexes with oxalosuccinic and oxalacetic acid, but the catalytic effect of these metals is considerably lower than in the case of Al^{+++}. It has been found that each of these various complexes has a characteristic absorption spectrum in the ultra violet region.

The authors also present spectral evidence for complex formation between Al^{+++} and oxalacetic acid and proposed that metal complexes are formed with the enol form of keto acids by the following steps:

$$\text{I} \qquad \text{keto acid} \rightleftharpoons \text{enol}$$

$$\text{II} \qquad \text{enol} + \text{cation} \rightleftharpoons \text{complex}$$

$$\text{III} \qquad \text{complex} \longrightarrow \text{keto acid} + CO_2 + \text{cation} \qquad (3)$$

In the same paper it was pointed out that Mn^{++} does not alter the absorption spectra of α-ketoglutaric and pyruvic acids.

Decarboxylation of oxalacetic acid in the presence of a great number of polyvalent cations has been measured manometrically by Speck at a temperature of 30°C, and pH-5 (5). Fig. 1 summarizes the effects of 14 different metal ions on the rate of decarboxylation of oxalacetic acid (5).

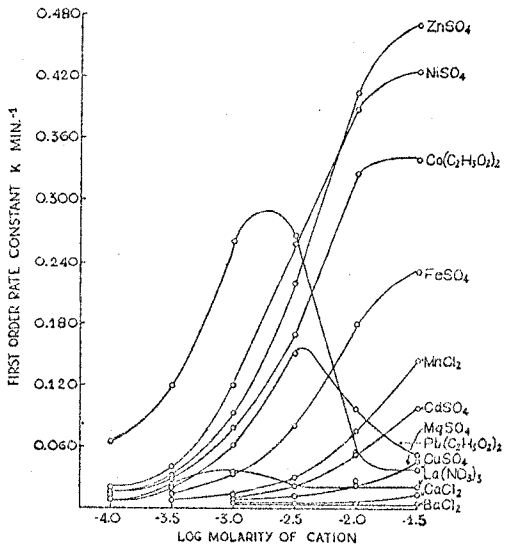

FIG. 1. Effect of various cations on the non-enzymatic decarboxylation of oxalacetate. Samples contained 0.1 M acetate, pH 5.0, 1 mg. of oxalacetic acid (equivalent to 160 μl. of CO_2), and metal salts in the concentrations indicated, in a total volume of 2.0 ml. Temperature 30°. In the absence of added polyvalent cation, the first order rate constant was 0.006 min.⁻¹.

Speck noted that, in agreement with Krebs, the effect of cations is independent of the nature of the anion combined with it. It has been shown that the decarboxylation reaction accelerated by metal ions, with exception of Fe^{+++} and Al^{+++}, follows first order kinetics.

P. Nossal reported (6, 8) the influence of the copper and iron on decomposition of oxalacetic acid by measuring CO_2 production in a standard Warburg apparatus. He has shown that decomposition of copper-oxalacetic acid complex is most rapid around pH-4, and that the rate diminshes on either side of that value. Above the pH 6 the decomposition is almost negligible.

Formation of the Fe^{+++} oxalacetate complex is not instantaneous as in the case of Cu^{++}, but usually reaches a maximum within two minutes after the addition of the metal ion. The rate of decomposition of the ferric com-

plex is lower than that of the Cu^{++} complex with oxalacetic acid.

Pedersen (9) studied the decarboxylation of oxalacetic acid promoted by Zn^{++} and Cu^{++}. He suggested that the catalysis may be explained by the spontaneous decarboxylation of a complex of the composition (M-OAA) with the spontaneous decarboxylation of the complex ($M\text{-}OAA^{+}$) contributing to the reaction.

His results are expressed by the following equation and numerical values are given in Table V.

$$M^{++} + OAA^{-} \overset{K_3}{\rightleftharpoons} M\text{-}OAA + H^{+}$$

$$M^{++} + OAA^{-} \overset{K_4}{\rightleftharpoons} M\text{-}OAA^{+} \qquad (4)$$

The velocity of decomposition was expressed by the following sum:

$$V = V_{spon.} + k_3(M\text{-}OAA) + k_4(M\text{-}OAA^{+})$$

$$V = V_{spon.} + k_3K_3(M^{++}).(OAA^{-}).(H^{+})^{-1} + k_4K_4(M^{++}).(OAA)^{-} \qquad (5)$$

Where K_3 and K_4 denote mass action constant and k_3 and k_4 respective rate constant.

TABLE V

Cupric and Zinc Ion Catalysis in the

Decarboxylation of Oxalacetic Acid at 37.0°C.

Ion	Ionic Strength m/l	k_3K_3	k_4K_4	K_3	K_4	$\frac{(Cu\text{-}OAA)}{(Cu^{++})(OAA^{=})}$
Cu^{++}	0.053	7.02	1.6	2.03	3.45	1.88×10^4
	0.104	5.76	1.31	1.74	3.31	1.25×10^4
	0.206	4.51	1.15	1.20	3.75	0.67×10^4
Zn^{++}	0.200	0.0419	0.145	....	....	....

Pedersen found that there is a linear relationship between the rate constants and the concentration of $ZnCl_2$ when the hydrogen ion concentration is constant and that the effect of the zinc ion increases with decreasing hydrogen ion concentration.

Gelles and co-workers (12 - 16) have investigated the catalytic activity and the nature of the chelate compounds formed by transition metals and oxalacetic acid, as well as the acceleration in the decarboxylation of oxalacetic acid by rare earth ions. The rate of decarboxylation has been expressed in terms of the concentration of the various species by the following equation:

$$\frac{d(CO_2)}{dt} = k_o(OAA) + k_1(OAA^-) + k_2(OAA^=) + k_c(M\text{-}OAA) \qquad (6)$$

where OAA, OAA^-, $OAA^=$ and M-OAA represent oxalacetic acid, its two anions and catalytically active complex respectively, and k_o, k_1, k_2 and k_c the corresponding first order rate coefficients, $k_{obs.}$ is related to the rate constant for the decomposition of the complex k_c and to the coefficient for the uncatalyzed reaction k_u by:

$$\frac{k_{obs.} - k_u}{X.C} = k_c \cdot K(H^+)^{-1} + \text{const.} \qquad (7)$$

where c is the concentration of the free metal, x the ionization constant of oxalacetic acid, H the hydrogen ion concentration and K the association constant for the complex M-OAA.

Table VI gives rate constants and thermodynamic association constants for the rare earth ions with oxalacetic acid at 25°C and ionic strength 0.22 (13).

TABLE VI

	La^{3+}	Cd^{3+}	Y^{3+}	Dy^{3+}	Lu^{3+}
$10^3/k_{obs.} - k_u$	1.11	3.36	3.27	4.05	7.42
$10^{-5}K_1$	1.8	3.5	4.3	4.6	7.5

The authors have shown that for diamagnetic ions a linear free energy relationship exists between the logarithms of the appropriate rate coefficients and the thermodynamic association constant.

Rate coefficients k_cK for transition metal ions have also been reported by Gelles (12) at 37°C (Table VII).

TABLE VII

Rate Coefficients k_cK for Oxalacetic Acid and Transition Metal Ions at 37°C.

Zn^{2+}	Cu^{2+}	Ni^{2+}	Co^{2+}	Mn^{2+}	Ca^{2+}
7.4	700	10.2	4.2	0.70	0.14

He pointed out that the catalytic rate constant reflects the interaction of metal ion and substrate in the transition state of decarboxylation and that the thermodynamic association constants are a measure of this interaction.

By using potentiometric and spectrophotometric methods, Gelles and Hay (14) investigated the role of chelate compounds in the decarboxylation

of oxalacetic acid and have proposed that the ketonic chelate compounds are the kinetically active species in decarboxylation. They have found that the chelate compounds which are formed are not entirely ketonic. On chelation with the metal ions, the maximum absorption of oxalacetic acid is shifted to the higher wavelength and the absorbance indexes are increased two or three fold. They accounted for the change of absorbance, during the decarboxylation, by the formation of a strongly absorbing enolic pyruvate intermediate which subsequently ketonizes.

Experimental results on keto-enol equilibria for the metal oxalacetate complexes calculated on the basis of the approximate data for the respective absorbance indexes are presented in Table VIII (14).

TABLE VIII

Keto-enol Equilibria for Metal Oxalacetate

Oxalacetate dianion ($OAA^{=}$) : 1.25×10^{-4} M

Metal ion (M) : 3.33×10^{-4} M

pH : 6.35

Metal ..... :	Ca^{++}	Mn^{++}	Co^{++}	Zn^{++}	Ni^{++}	Cu^{++}
Enolic complex % :	5	6	13	15	22	40

A detailed study of the catalysis of the decarboxylation of oxalacetic acid by transition metal ions at 36.9°C and various hydrogen ion concentrations at ionic strength 0.1 has been reported by Gelles and Salama (15,16). They reported catalytic rate coefficients $k K_{MA}$ which provide a measure for the effect of metal ion on the rate of the reaction. A parallelism between the rate coefficient kK_{MA} and association constants K_{MA} was found.

Table IX gives the experimental values of the rate constants for chelate compounds M-OAA.

TABLE IX

The Rate Constants for Chelate Compounds M-OAA at 36.9°C and Ionic Strength 0.1

	Ca^{++}	Mn^{++}	Co^{++}	Zn^{++}	Ni^{++}	Cu^{++}
kK_{MA}	0.14	0.65	4.8	7.6..	10.7	706
10^2 k approx.	0.24	0.65	2.4	3.1	2.3	6.6

The enzymatic decarboxylation of oxalacetic acid was discovered by Krampitz and Werkman (17). The enzyme from Micrococcus lysodeikticus requires catalytic amounts of Mg^{++} or Mn^{++} and it was found that the Mn^{++} is much more active than Mg^{++}. There are a great number of published papers dealing with enzymatic decarboxylation of oxalacetic acid, but kinetic studies and the mechanisms of these reactions are still scarce (29-33).

Westheimer and collaborators (18,19) studying the enzymatic and the metal-ion-promoted decarboxylation of oxalacetic acid, proposed the following mechanism for the metal-ion-catalyzed decarboxylation by studying the decarboxylation of the dimethyloxaloacetic acid:

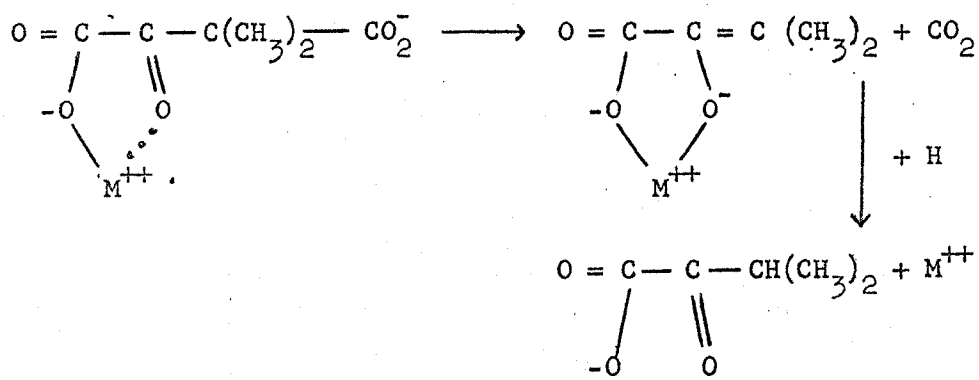

(8)

This catalysis by metal ion has served as a model for the enzymatic reaction (34).

Isotope effects in enzymatic and metal catalyzed decarboxylation of oxalacetic acid have been studied by Seltzer, Hamilton and Westheimer (35). It is shown that the enzymatic decarboxylation proceeds less rapidly in D_2O than in H_2O, whereas the rate of the manganese catalyzed decomposition of oxalacetic acid is unaffected by these changes of solvent. The relative rates of the enzymatic decarboxylation of oxalacetic acid in H_2O and in D_2O are illustrated in Figure 2.

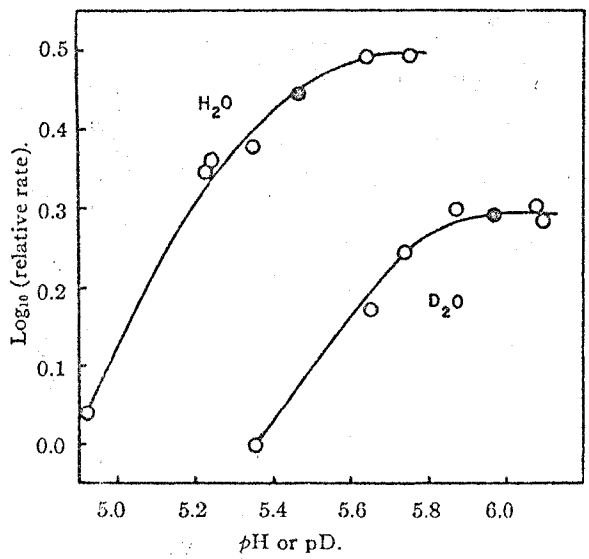

Fig. 2.—Rates of decarboxylation of oxalacetic acid in H_2O and D_2O. Open circles for glutarate buffer; filled circles for acetate buffer.

Possible inhibition of decarboxylation reaction by CO_2 of the enzymatic and manganese catalyzed reaction have also been reported by these authors. The results show that CO_2 does not appreciably inhibit the metal ion promoted reaction and that the inhibition of the enzymatic reaction is about 40% with one atmosphere of CO_2.

In living cells magnesium ion plays an important role as an activating ion in many enzymatic reactions, among them the decarboxylation of oxalacetic acid which is an essential step in metabolism. Westheimer (34) has pointed out the importance of metal ions in the decarboxylation indicating the close analogy existing between the mechanism of the metal-ion and enzyme catalyzed reactions. Quantitative studies on the kinetics of the decarboxylation of oxalacetic acid have been carried out on other metal ions but the influence of magnesium ion has been neglected. Therefore, we have investigated the magnesium-ion catalyzed decarboxylation of oxalacetic acid to further the understanding and parallelism between the enzymatic and metal ion promoted reaction.

The result of the present study shows that magnesium-ion has a low catalytic activity compared to the other divalent metals, but still it involves a change of absorption spectrum indicating the formation of a chelate. The rate of decarboxylation of oxalacetic acid was found to depend on both the magnesium-ion and pH(pD). The range of the optimal activity (pH 5 to 6) for the magnesium-ion-catalyzed reaction corresponds to the range for the enzymatic decarboxylation (32, 35, 36, 37, 38).

II. EXPERIMENTAL

A. Methods

The following materials were commercial preparations: oxalacetic acid (OAA) (Sigma Chemical Co.), $MgCl_2.6H_2O$ reagent grade, Tris(hydroxymethyl)aminomethane (Tris) was primary standard grade. The D_2O (99.78 atom % excess D) was purchased from the Atomic Energy Commission of Canada Limited, Ottawa.

Measurements of pH and pD of each reaction mixture were made at the end of the experiment with a Beckman Model G pH meter standardized with pH 7 buffer. When D_2O was used as a solvent the measurements were made with the same glass and calomel electrodes and the pD was calculated by adding 0.4 units to the observed meter reading (39). The buffer system used was a Tris-acetate mixture. To adjust the pH, 1 molar basic Tris and 1 molar acetic acid were mixed in the proper proportions. For the D_2O systems all the reagents were made up in D_2O.

Absorption spectra were measured with a Bausch and Lomb Spectronic 505 spectrophotometer. Rates of reaction were followed either in the Beckman DU spectrophotometer or on the Gilford Instrument Model 2000 Absorbance Recorder (Beckman monochromator). The temperature of the reaction cell was kept at $25.0 \pm 0.2^{\circ}C$ by a water-cooled circulating bath.

B. Results

Kinetic experiments at $25.0^{\circ}C$ were measured over a period of three half-times for the spontaneous decarboxylation of oxalacetic acid, and followed to the end of the reaction for the magnesium-ion-catalyzed reaction. The observed rate constants were calculated graphically from the slopes of the first order plots and from the equation:

$$k_{obs} = \frac{2.303}{t} \log \frac{A_o - A_e}{A_t - A_e} \qquad (9)$$

where A_o is the absorbance at zero time, A_e is the absorbance at equilibrium, A_t is the absorbance at time t, t is the time in minutes and k_{obs} is the observed rate constant (min^{-1}).

The observed first order rate constants for the spontaneous decarboxylation of oxalacetic acid measured at 255 mμ are plotted as a function of pH and pD in Figure 3. The bell-shaped curve for the D_2O system shows a shift to a higher pD value of about 0.6 pH (pD) units. For the spontaneous decarboxylation of oxalacetic acid the buffer concentration definitely has an effect on the observed rate constant. Beyond a concentration of 0.7 molar, however, further increases of buffer had no significant effect on the observed rate constant. For this reason the reactions were followed within the range of this plateau of buffer effect. At the optimal activities of decarboxylation (cf. Fig. 3), however, the deviations due to buffer effects are accentuated, and deviations from the first order plot are observed after a half-time of reaction. In the D_2O system from pD 6 to 8 the observed rates were corrected for initial ketonization. The kinetic data for spontaneous decarboxylation are compared in Table IV. For the magnesium-ion-catalyzed decarboxylation the buffer effects are negligible compared to the catalytic effect of the metal ion.

The magnesium-ion-catalyzed decarboxylation of oxalacetic acid was measured spectrophotometrically by the decrease of absorption at 278 mμ and 255 mμ depending on the concentration of magnesium ion used. The spectrum of oxalacetic acid as a function of magnesium ion concentration is plotted in Figure 4. It appears that only a fraction of the actual

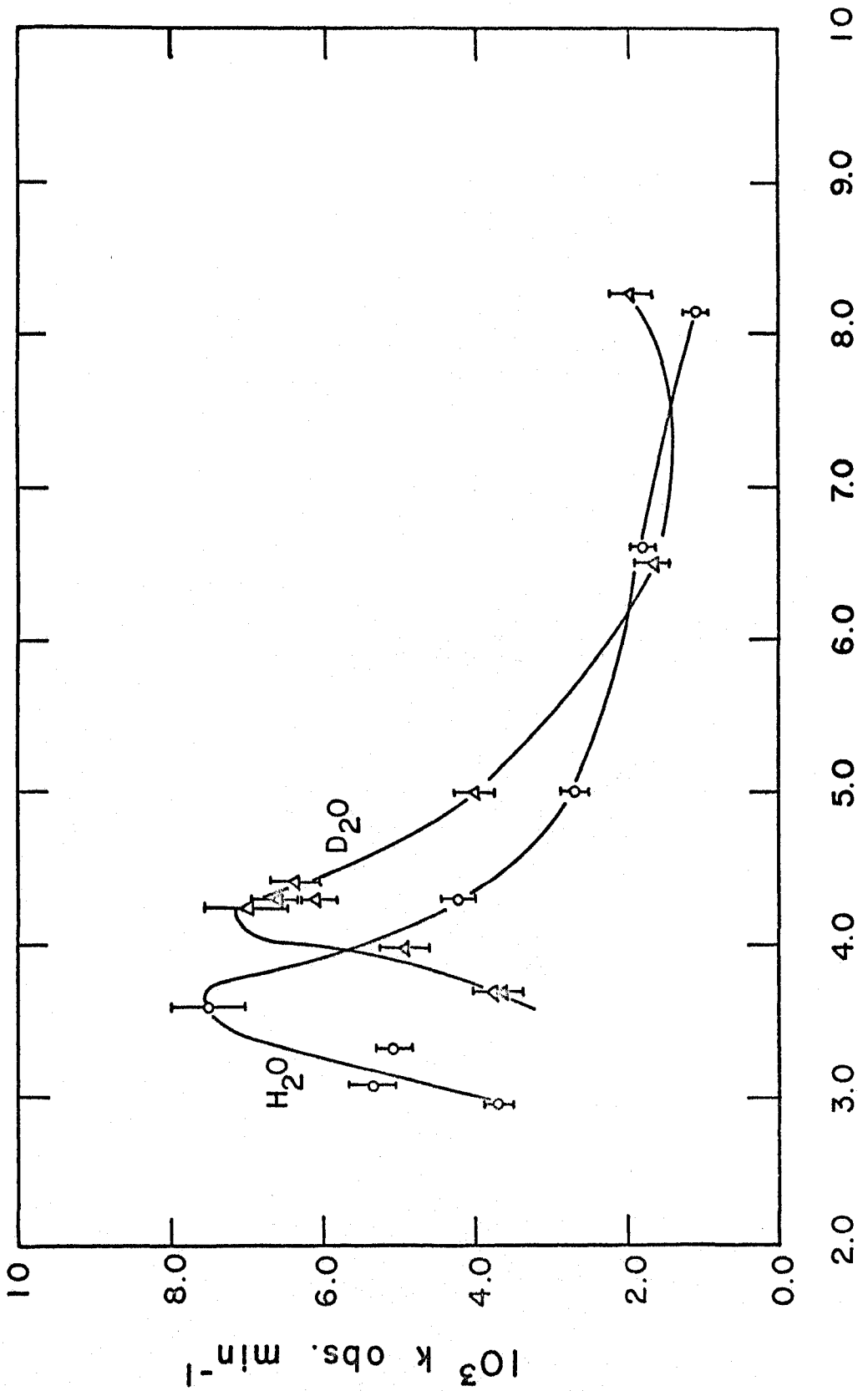

Fig. 3.

Figure 3 Spontaneous Decarboxylation of Oxalacetic Acid

Legend: Each cuvette (0.5 cm light path) contained $\sim$ 2 x 10^{-4} M oxalacetic acid and 1.0 M Tris-acetate buffer of the appropriate pH made up in H_2O or D_2O. Solid oxalacetic acid was added last and its concentration measured immediately by its absorption at 255 mμ. The zero time absorbance was determined by extrapolation of the plot of absorbance versus time.

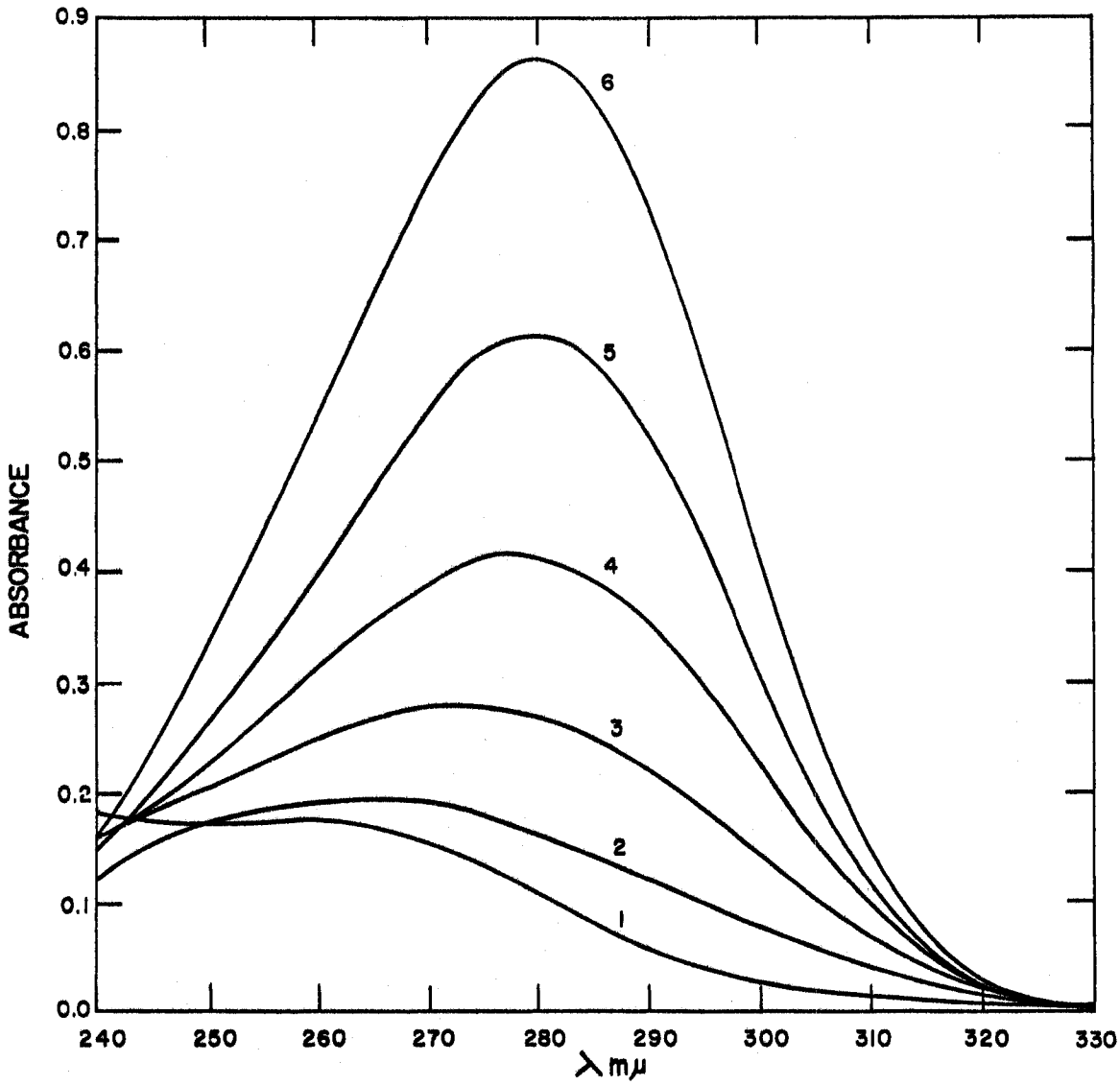

Fig. 4.

Figure 4 The Spectra of the Magnesium Chelate as a Function of Magnesium Ion Concentration

Legend: Solutions were prepared in 25 ml volumes adjusted to pH 7.40 ± 0.04 with Tris-acetate buffer 0.5 M and measured in 1.0 cm light path cuvettes within 2 minutes. The concentration of oxalacetic acid was 1.9×10^{-4} M. Magnesium chloride concentrations for the curves were: (1) 0.000, (2) 0.012, (3) 0.04, (4) 0.08, (5) 0.20, (6) 0.40 molar, giving a molar ratio of $Mg^{++}/OAA^{=}$ of 0, 64, 212, 424, 1060, 2120 respectively.

concentration of magnesium chloride added takes part in the effective formation of the complex with oxalacetate, probably because of the extensive hydration of the magnesium ion. It was found that in order to bind all the oxalacetate in a 1:1 complex (cf. Fig. 4) the molar ratio of magnesium to oxalacetate had to be greater than 10^3. Therefore, the effect of magnesium ion concentration can be considered at two levels.

At concentrations below 0.1 molar magnesium chloride (concentration of oxalacetic acid 2×10^{-4} M) there was found a linear relationship between the observed rate constant and the concentration of metal ion. The rate constant is low and shows no pH effect (cf. Fig. 5a,b,6a,b). The presence of magnesium ion causes only a slight intensification of the absorption spectra but no shift in the maximum of absorption. The observed rate constant measured spectrophotometrically at pH 5, 25°C is in the same order of magnitude as the constant measured by CO_2 evolution (5, 10) at pH 5, 30°C.

At concentrations above 0.1 molar magnesium chloride there is a change of the intensity of the integral absorption and a shift of the maximum to a higher wavelength (280 mμ). The reaction is strongly pH dependent (cf. Fig.5a,b) and the observed higher rate constants (at pH 5) are of the same order of magnitude as found for much lower concentrations of Cu^{++} and Mn^{++} and other divalent cations catalyzed reactions (5). The absorbance at 280 mμ of the magnesium-oxalacetate complex as a function of pH and pD in the presence of excess magnesium ion is plotted in Figure 7.

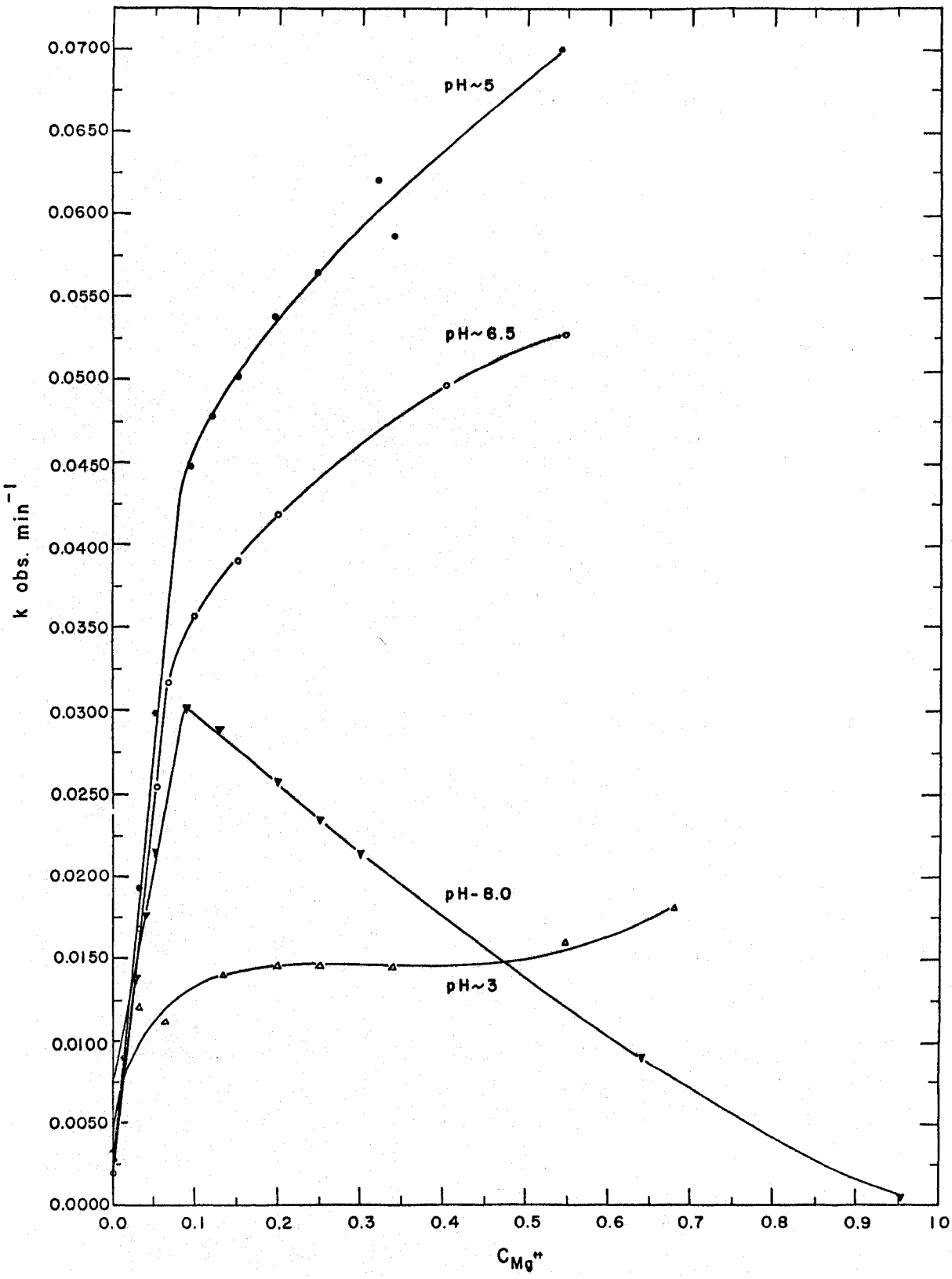

Fig. 5a.

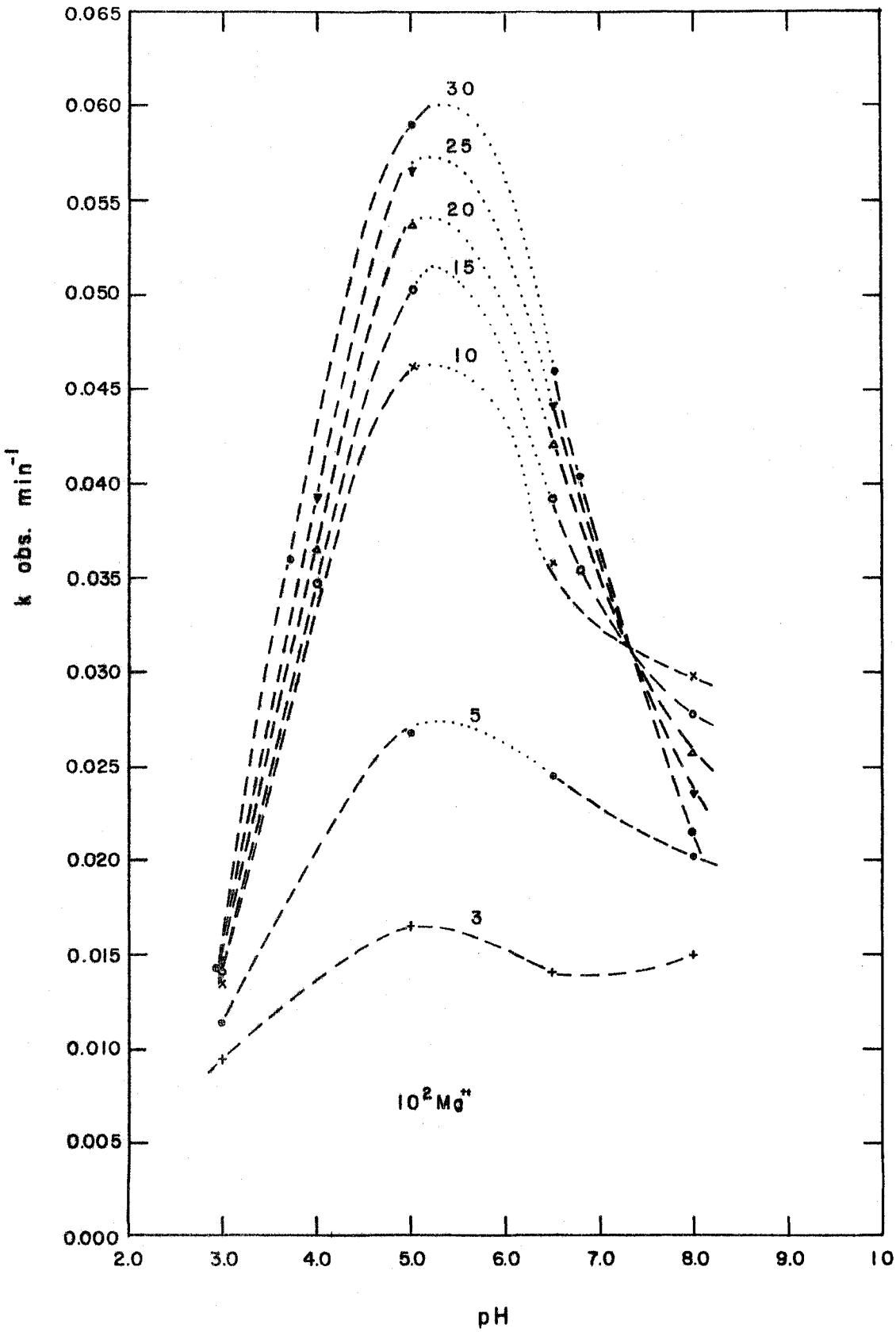

Fig. 5b.

Figure 5a,b. The Observed First Order Rate Constant of Decarboxylation as a Function of pH and Magnesium Ion Concentration (278 mμ)

Legend: Each cuvette (0.5 light path) contained 0.3 - 0.5 M Tris-acetate buffer of the appropriate pH, ~ 2 x 10^{-4} M oxalacetic acid, varying concentrations of $MgCl_2$, 3, 5, 10, 15, 20, 25, 30 each x 10^{-2} M.

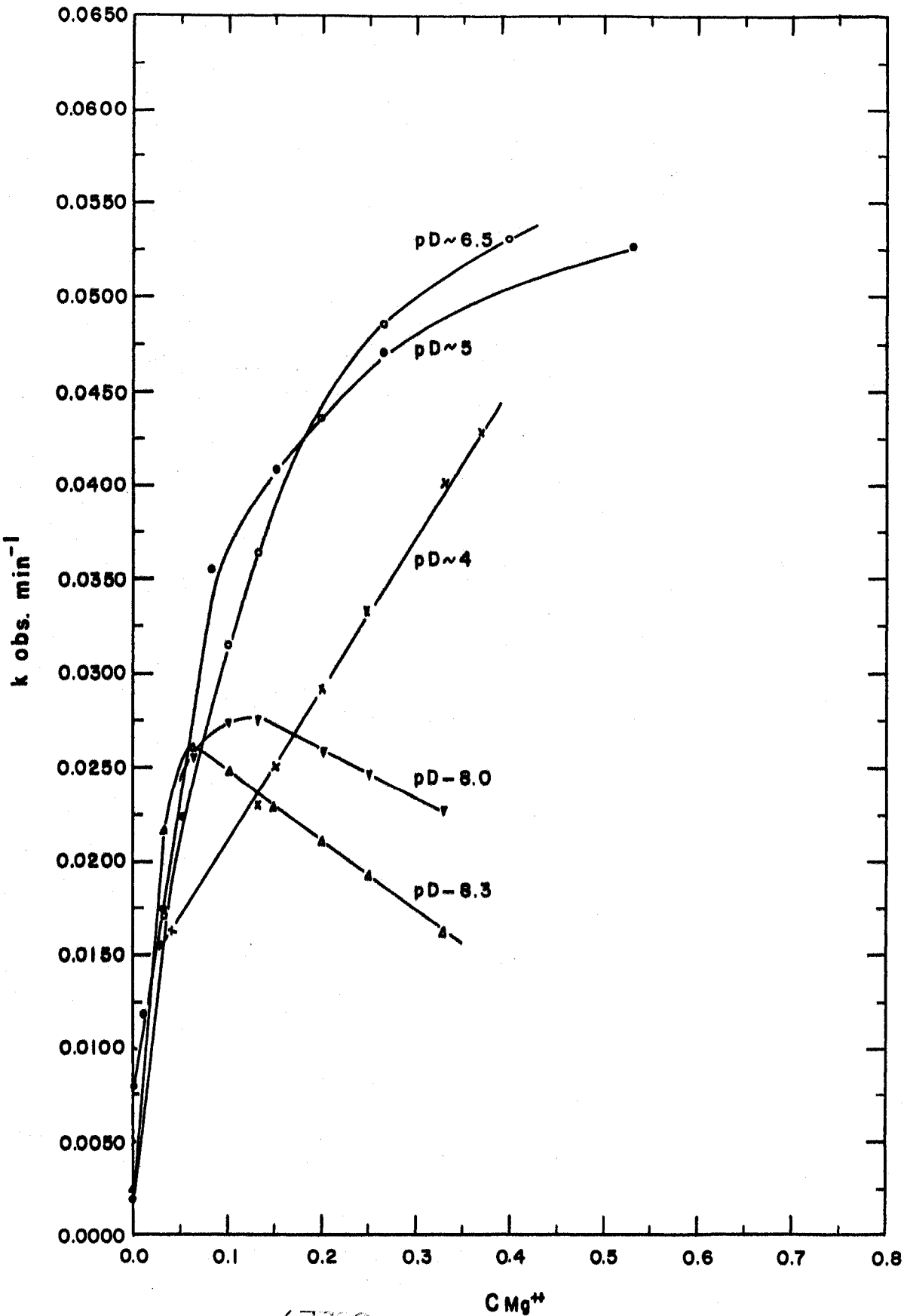

Fig. 6a.

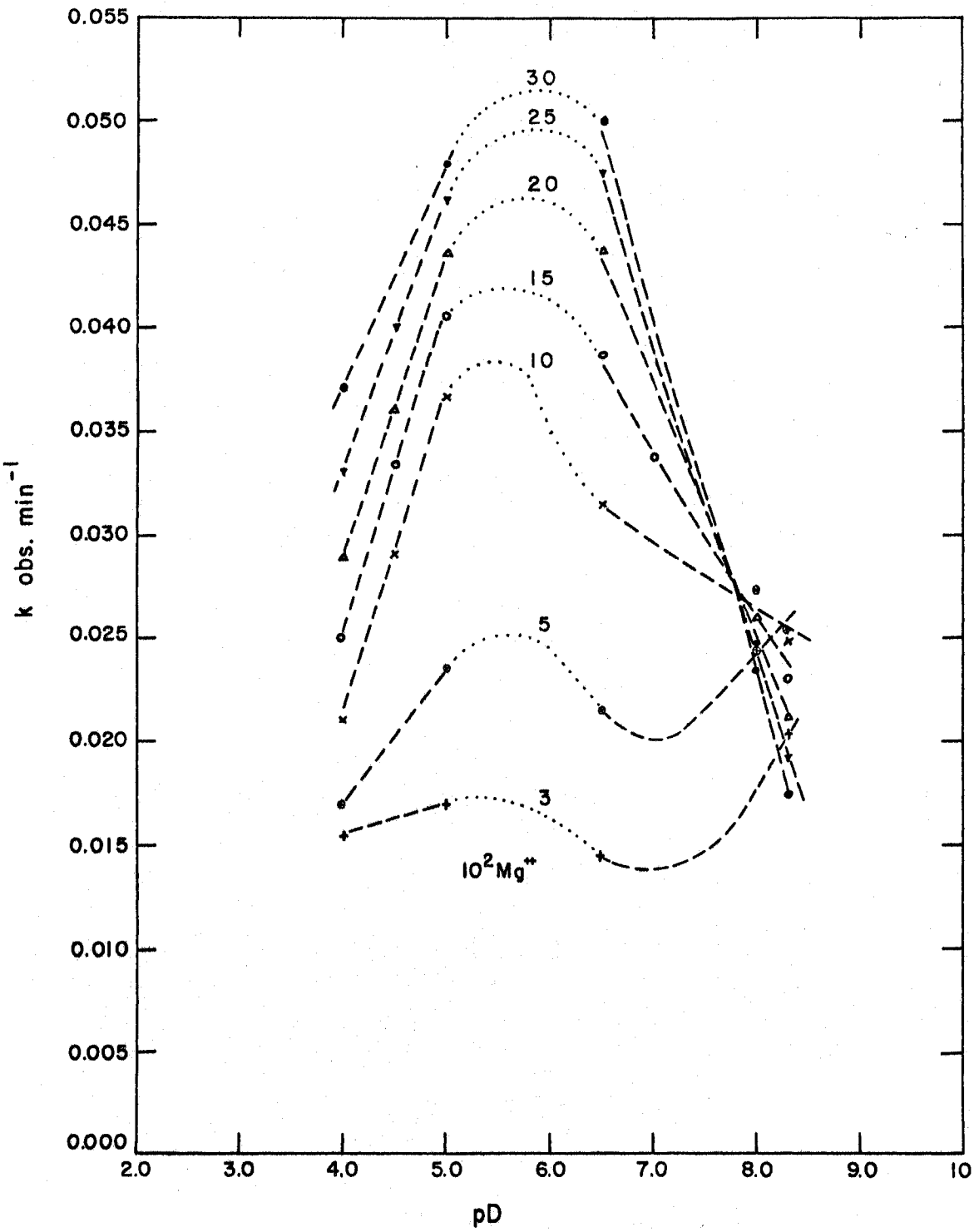

Fig. 6b.

Figure 6a,b The Observed First Order Rate Constant of Decarboxylation as a Function of pD and Magnesium Ion Concentration (278 mμ)

Legend: Each cuvette (0.5 cm light path) contained 0.3 - 0.5 M Tris-acetate buffer of the appropriate pD, ~ 2 x 10^{-4} M oxalacetic acid, varying concentrations of $MgCl_2$, 3, 5, 10, 15, 20, 25, 30 each x 10^{-2} M.

The observed first order rate constants are summarized in Table X and are partially plotted as a function of pH at varying concentrations of magnesium ion in Figure 5b. The bell-shaped activity plot shows a maximum rate in the range of pH 5 to 6, with a convergence of the observed rate constant (isokinetic point) at pH 7.4. In order to reach the isokinetic point the molar ratio of magnesium ion to oxalacetate must exceed 10^3. The rate of decarboxylation was also measured as a function of pD at varying magnesium ion concentrations (Table XI) and plotted in Figure 6a,b. The isotope rate effect of the observed first order rate constants at the isokinetic point (pH 7.4, pD 7.8) k_{H_2O}/k_{D_2O} is 1.1 ± 0.08.

The absorbancy index of the keto form of the magnesium-oxalacetate complex (a_K) in Tris-acetate buffer was calculated from kinetic and spectrophotometric measurements. On the basis of the kinetic experiments it is assumed:

(1) that the maximum concentration of the active species, the keto form of the magnesium-oxalacetate complex (C_K), exists at pH 5.5, since the activity is maximal at pH 5.5 (Fig. 5b).

(2) that the concentration of the active species is reduced to one-half its maximal concentration as the observed rate decreases to one-half of its maximal value as a function of pH. This decrease to 50% activity was found to occur at pH 7.4 (isokinetic point) for any given magnesium ion concentration.

On the basis of the spectrophotometric measurements (Fig. 7) made at greater than 1000 fold excess of magnesium ion as a function of pH, it is assumed:

(3) that the enol form of the magnesium-oxalacetate complex predominates at pH 9.0.

Under such conditions, the approximate value for the absorbancy index of the enol form of the magnesium-oxalacetate complex (a_E) can be calculated to be 8.05×10^3. The absorbancy index for the keto form of the complex (a_K) can be then calculated from the following basic equations at pH $\geqslant 5.5$, 1 cm light path: [Cf Appendix I).

$$C_T = C_E + C_K = C_T' = C_E' + C_K' \tag{10}$$

$$A_T = a_E c_E + a_K c_K \tag{11}$$

$$A_T' = a_E c_E' + a_K c_K' \tag{12}$$

$$C_K' = \frac{C_K}{2} \tag{13}$$

solving for a_K:

$$a_K = \frac{a_E(A_T + C_T a_E - 2A_T')}{A_T + C_T a_E + 2A_T'} \tag{14}$$

where C_T is the total concentration of the complex and C_E and C_K are the concentrations of the enol and keto forms of the complex and A_T is the total absorbance at 280 mμ (pH 5.5). The primed numbers refer to the values at one-half maximal activity (pH 7.4). From these equations the molar absorbancy index for a_K is 5.38×10^2 in H_2O. For the D_2O system a_E is 10^4 and a_K is 6.3×10^2.

The above assumptions are supported by other evidence. Calculations of the percentage of keto and enol forms of the complex as a function of pH (pD) using the above absorbancy indexes show that at pH 7.4 (pD 7.8), which appears to be the pK for the keto-enol complex, there is a

1:1 ratio of the concentrations of the keto to enol complexes (Table XII and Figure 8). Further support comes from the determination of the over-all association constant for the magnesium-oxalacetate complex at pH 7.4 in Tris-acetate buffer at constant ionic strength of 0.4. The calculations (40, 41) are based on the following equation, (Equation 15) where the magnesium ion concentration is much greater than the oxalacetate concentration and:

$$\frac{C_{Mg^{++}} \; C_{OAA^{=}}}{A} = \frac{1}{Ka_C} + \frac{C_{Mg^{++}}}{a_C} \qquad (15)$$

where $C_{Mg^{++}}$ and $C_{OAA^{=}}$ are the concentrations of magnesium ion and the di-anion of oxalacetic acid, A is the total absorbance at 280 mμ, a_C is the absorbancy index of the complex and K is the over-all association constant. The results are plotted in Figure 8. Based on the over-all absorbancy index of the complex of 3.85×10^3 and on the calculated absorbancy indexes for the keto and enol forms of the complex, the keto complex concentration at pH 7.4 is also found to be 51%. The over-all association constant K is 13.7.

The rate of formation of the magnesium-oxalacetate complex at pH 7.0 was compared to the rate of enolization of oxalacetate and is shown in Figure 9. The formation of the magnesium complex could only be observed at low concentrations of magnesium ion where the rate of decarboxylation is relatively slow.

Table X Observed First Order Rate Constant for the Mg^{++} Catalyzed Decarboxylation of Oxalacetic Acid in H_2O

pH	10^2 Mg^{++}	$\lambda_{m\mu}$	10^2 k observed min^{-1} Slope Value	Calc'd. Value	10^2 av. $\pm \frac{\Sigma v}{n}$
3.02	3	255	0.95	0.98	± 0.06
3.03	5	255	1.14	1.16	0.05
3.08	10	255	1.35	1.36	0.05
2.98	15	255	1.41	1.42	0.05
2.98	20	255	1.45	1.47	0.10
2.97	25	255	1.46	1.48	0.11
2.98	30	255	1.47	1.49	0.11
2.98	34	255	1.47	1.58	0.11
2.91	55	255	1.62	1.74	0.11
2.90	68	255	1.83	1.87	0.05
5.08	1.3	255	0.90	0.91	0.02
5.08	3	255	1.95	2.00	0.07
5.01	5	255	2.99	2.98	0.08
5.00	10	278	4.60	4.66	0.16
4.98	15	278	5.03	5.10	0.10
4.97	20	278	5.38	5.45	0.11
5.01	25	278	5.66	5.78	0.15
4.98	32	278	5.93	6.21	0.37
4.80	34	278	5.87	5.92	0.10
4.70	54	278	7.00	7.20	0.26
6.47	3	255	1.68	1.62	0.07
6.43	5	255	2.45	2.50	0.05
6.47	6.7	255	3.17	3.16	0.06
6.50	10	278	3.57	3.63	0.08
6.49	15	278	3.92	3.96	0.07
6.53	20	278	4.19	4.17	0.09
6.48	25	278	4.42	4.41	0.05
6.50	30	278	4.62	4.65	0.10
6.48	40	278	4.99	4.96	0.08
6.41	55	278	5.36	5.46	0.10
8.00	2.6	255	1.39	1.36	0.08
8.00	3	278	1.60	1.52	0.05
8.00	4	278	1.75	1.70	0.05
8.00	5	278	2.16	2.17	0.04
8.00	10	278	2.87	2.89	0.05
8.01	15	278	2.78	2.76	0.05
8.00	20	278	2.58	2.56	0.04
8.01	25	278	2.36	2.34	0.05
8.00	30	278	2.15	2.13	0.05
8.01	64	278	0.92	0.92	0.10
8.00	96	278	0.52	0.54	0.18

Table XI Observed First Order Rate Constant for the Mg^{++} Catalyzed Decarboxylation of Oxalacetic Acid in D_2O

pD	10^2 M Mg^{++}	$\lambda m\mu$	10^2 k observed min^{-1} Slope Value	Calc'd. Value	10^2 av. $\pm \frac{\Sigma v}{n}$
4.09	3	255	1.56	1.49	0.07
4.09	4	255	1.64	1.60	0.05
4.01	5	255	1.70	1.72	0.06
3.99	10	255	2.30	2.29	0.08
4.00	15	278	2.51	2.56	0.10
4.01	20	278	2.90	2.85	0.08
3.98	25	278	3.31	3.26	0.07
4.00	30	278	4.03	3.91	0.10
3.95	37	278	4.30	4.29	0.14
4.91	1.4	255	1.19	1.19	0.04
5.00	3	255	1.72	1.70	0.07
4.95	5	255	2.41	2.37	0.04
4.85	8	278	3.57	3.68	0.24
5.01	10	278	3.66	3.76	0.10
5.00	15	278	4.05	4.08	0.08
5.01	20	278	4.37	4.47	0.10
4.95	26	278	4.73	4.85	0.13
4.98	30	278	4.81	4.90	0.15
4.85	53	278	5.26	5.17	0.23
4.78	66	278	6.13	6.02	0.16
6.51	3	255	1.45	1.50	0.08
6.60	3.4	278	1.71	1.74	0.03
6.50	5	278	2.15	2.12	0.10
6.50	10	278	3.15	3.20	0.05
6.50	13	278	3.64	3.65	0.05
6.51	15	278	3.87	3.90	0.05
6.52	20	278	4.37	4.32	0.08
6.50	25	278	4.87	5.01	0.20
6.50	30	278	5.10	5.09	0.15
6.40	40	278	5.34	5.36	0.02
8.01	3	278	1.75	1.70	0.05
8.00	6	278	2.56	2.54	0.03
8.01	10	278	2.70	2.75	0.70
7.99	15	278	2.73	2.75	0.05
7.98	20	278	2.60	2.61	0.05
8.00	25	278	2.47	2.45	0.06
8.00	30	278	2.35	2.30	0.08
7.99	33	278	2.18	2.19	0.05
8.31	5	255	2.61	2.66	0.08
8.34	3	278	2.18	2.14	0.05
8.30	10	278	2.48	2.37	0.10
8.31	15	278	2.30	2.29	0.05
8.30	20	278	2.12	2.10	0.06
8.32	25	278	1.93	1.88	0.10
8.30	30	278	1.64	1.59	0.10

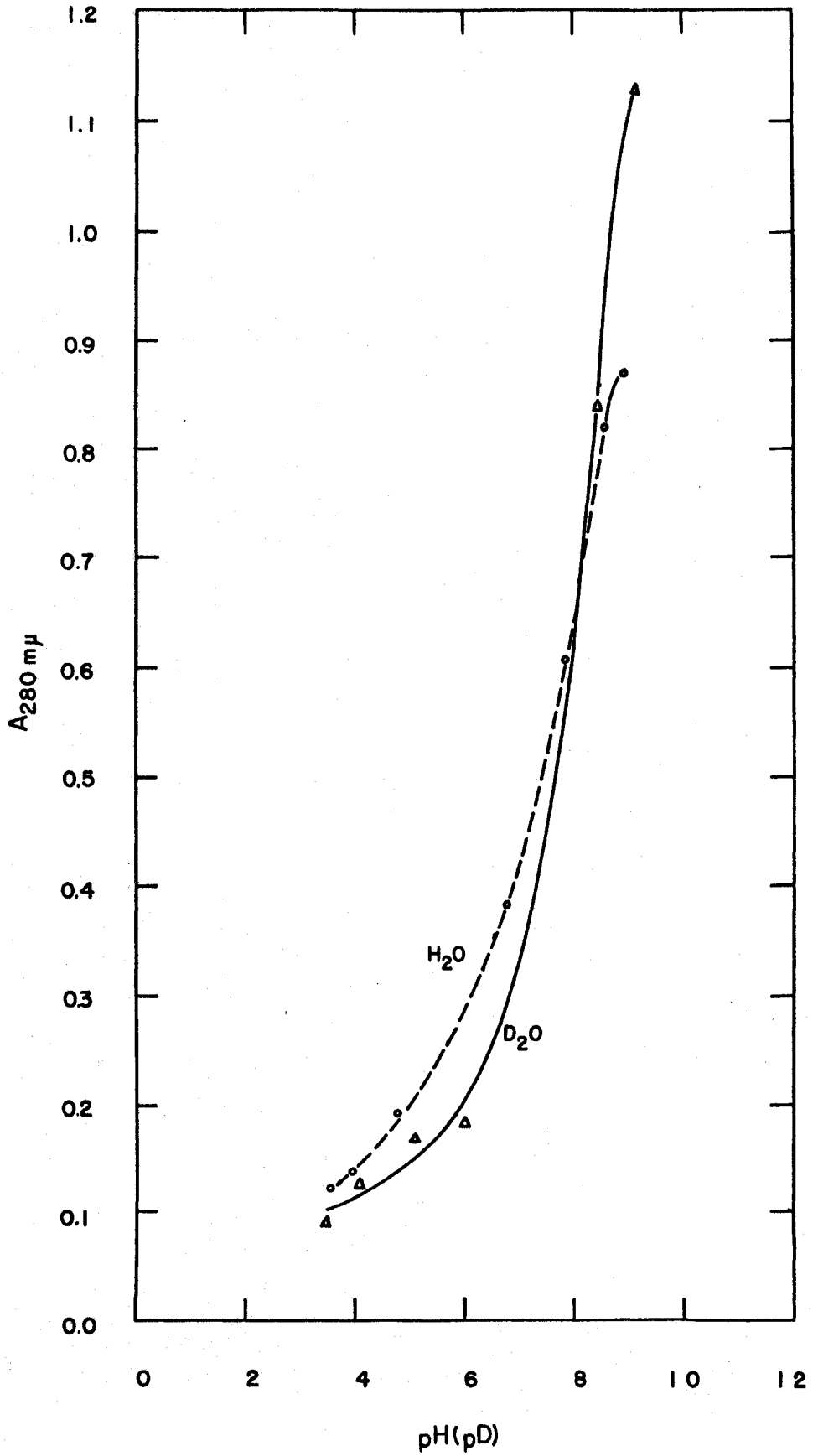

Fig. 7.

Figure 7 The Absorbance at 280 mμ of the Magnesium-Chelate as Function of pH and pD

Legend: For the H_2O system: solutions of 1.08×10^{-4} M oxalacetic acid, 0.2 M $MgCl_2$ and 0.1 M Tris-acetate buffer of the appropriate pH were made up to 25 ml in H_2O. Measurements were made within 1 - 1.5 min after each preparation in 1.0 cm light path cuvettes. For the D_2O system: $MgCl_2$ hydrated with heavy water was prepared by partial dehydration at 98°C of the hexahydrate and dissolving in D_2O and repeating. Solutions of 1.14×10^{-4} M oxalacetic acid, 0.2 M $MgCl_2$ and 0.1 M Tris-acetate buffer of the appropriate pD were made up to 10 ml in D_2O and measured as above.

Table XII Keto-Enol Equilibrium for Magnesium-Oxalacetate Complex

a)

pH	A_T 280 mμ	Approx. Per cent $C_K \pm 1\%$	$C_E \pm 1\%$
5.5	.250	76	24
6.0	.290	71	29
7.0	.410	56	44
7.4	.490	50	50
8.0	.680	23	77
>9		→ 0	→ 100

b)

pD	A_T 280 mμ	Approx. Per cent $C_K \pm 2\%$	$C_E \pm 2\%$
6.0	.190	89	11
7.0	.320	76	24
7.8	.580	52	48
8.0	.670	44	56
>9		→ 0	→ 100

Legend: Values are calculated using equation 14 and data from Figure 7.

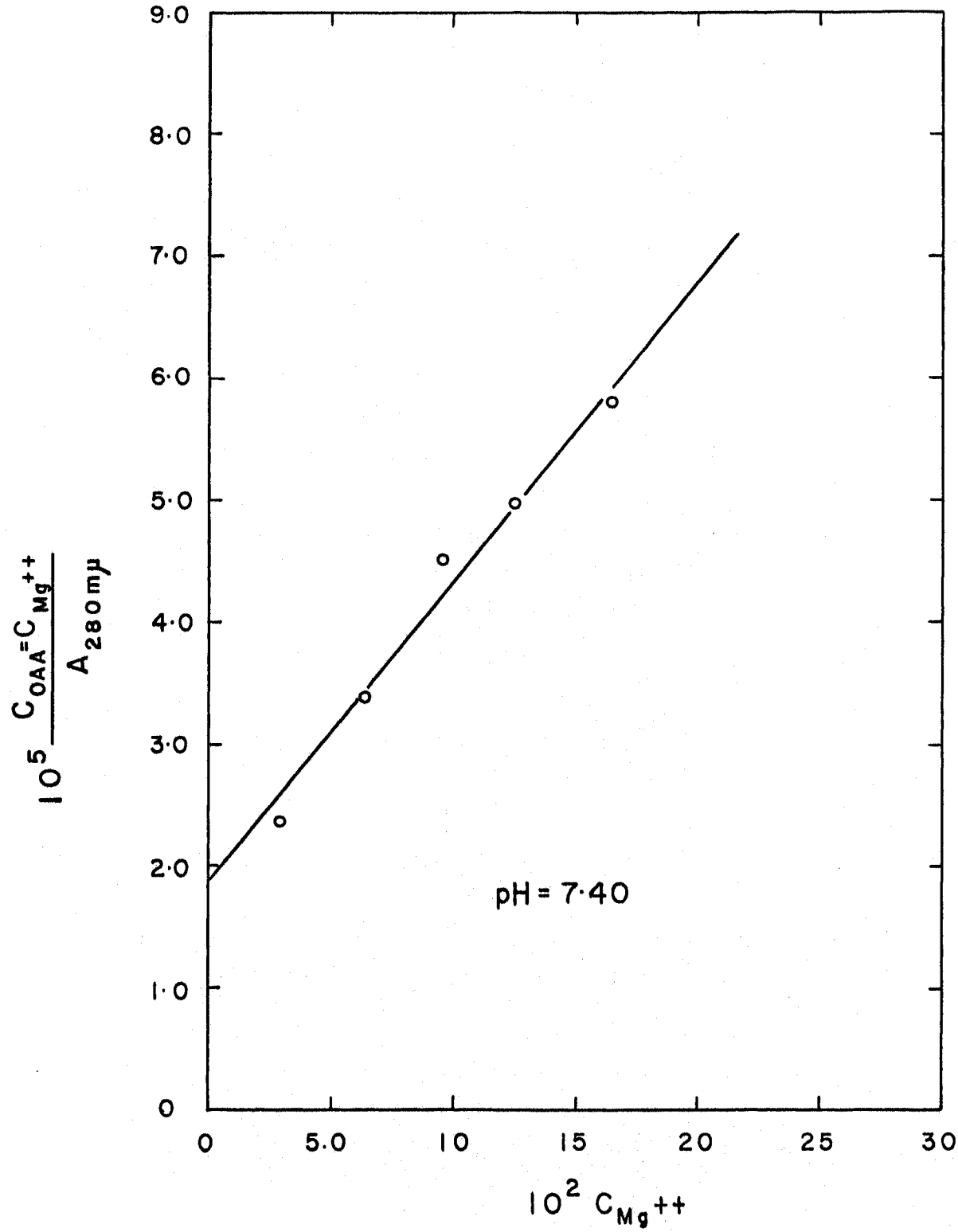

Fig.8.

Figure 8 Scott's Plott (18) for the Over-all Association Constant for the Magnesium-Chelate

Legend: Solutions of 8.66×10^{-5} M oxalacetic acid, varying concentrations of magnesium chloride, KCl to adjust the ionic strength to 0.4 and $\sim$0.05 M Tris-acetate of the appropriate proportions to give a resultant pH of 7.40 ± 0.02 were made up to 50 ml H_2O. Measurements were made at 280 $m\mu$ 2 min after preparation of the solution in 1.0 cm light path cuvettes. For magnesium chloride concentrations of 3.20, 6.38, 9.57, 12.76, 16.74, each $\times 10^{-2}$ molar the absorbancies at 280 $m\mu$ were 0.116, 0.163, 0.183, 0.222, 0.230 respectively.

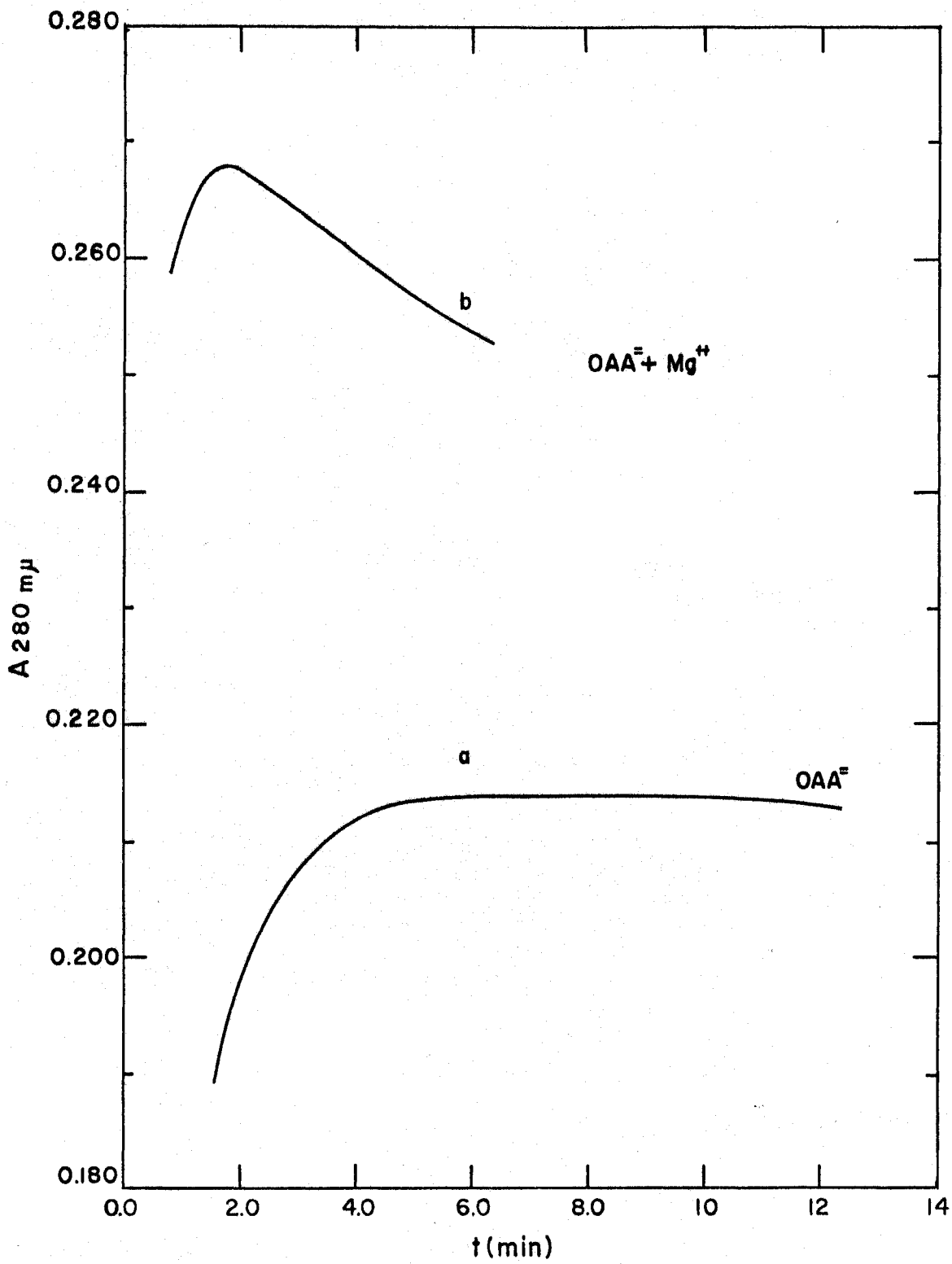

Fig. 9.

Figure 9 Formation of the Magnesium-Chelate

Legend: Solution (a) with 1.6×10^{-4} M oxalacetic acid was made up to 25 ml in 0.05 M Tris-acetate buffer, pH 7.10. Solution (b) with 1.6×10^{-4} M oxalacetic acid and 2.4×10^{-3} M $MgCl_2$ was made up to 25 ml in 0.05 M Tris-acetate buffer, pH 7.14. The reactions were followed in a 1.0 cm light path cuvette.

III. DISCUSSION

The spontaneous decarboxylation of oxalacetic acid follows a bell-shaped activity curve with a maximum of activity at about pH 3.6. The correspondence of the curve to the dissociation constants of oxalacetic acid of pK 2.5 and 4.5 (depending on ionic strength) indicates that the species that decarboxylates is the mono-anion of the carboxyl β to the carbonyl group. The α-carboxyl group in the protonated form can aid in the decarboxylation through a cyclic hydrogen bonded intermediate:

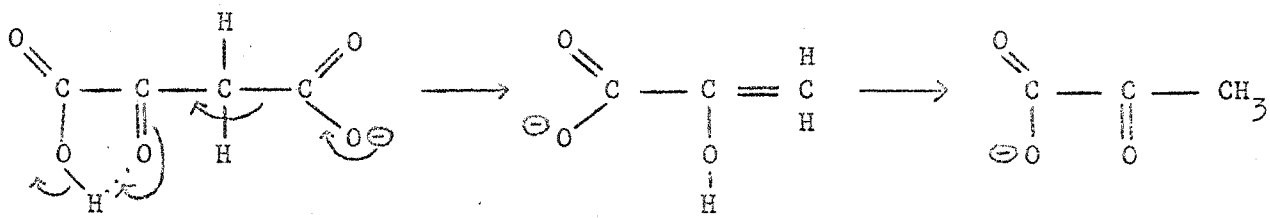

+ CO_2 (16)

At pH 3.5 the keto form of oxalacetic acid is the predominate species (42) When the maximum activity is reached at about pH 3.5 the first dissociation (pK_1 2.5) is virtually complete (43). The rate of the reaction begins to decrease as the pH increases to where the second carboxyl group starts to dissociate (pK_2 4.5) and reaches a minimum rate when the fully dissociated form is predominant. The anion of pyruvic acid with a pK of about 2.5 depending on ionic strength is the product at pH 3.5. The activity plot as a function of pH (Figure 3) confirms the kinetic studies of Pedersen (9) and Gelles(11) who conclude that oxalacetic acid in the form with the anion β to the carbonyl decarboxylates much faster than in the undissociated form (44 times).

The shift of the bell-shaped activity curve in D_2O to higher pD values can be interpreted as an increase in the two pK groups of the deuterated oxalacetic acid (44):

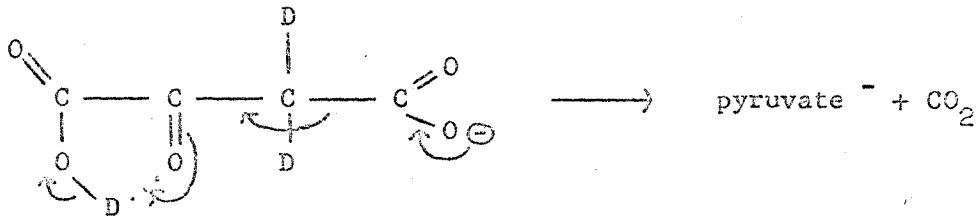

(17)

The shift of the maximum involves a step in which the rate depends on the increased stability of the deuterium bond. This behaviour gives further and direct evidence that the cyclic mono-anion intermediate is the active species that decarboxylates (10).

The magnesium-ion-catalyzed decarboxylation of oxalacetic acid approximates a bell-shaped curve with a maximum rate between pH 5 and 6 (Fig.5b). At pH 3 (Fig 5a) increases of magnesium ion above a molar ratio of magnesium ion to oxalacetate of 10^3 have no effect on the observed rate constant. At this pH there was found an intensification of the absorption at 260 mμ but no shift of the peak to 280 mμ. This can be interpreted as the formation of the saturated mono-ligand complex which has a slower rate of decarboxylation:

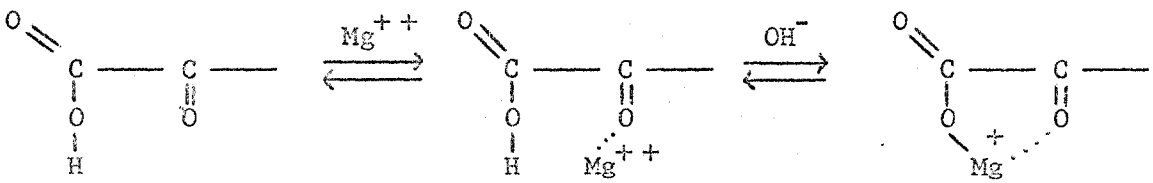

(18)

The activity increases over the range of pH where the second carboxyl group of oxalacetic acid begins to dissociate. In this range the magnesium ion is free to form the chelate with oxalacetate.

At the maximum activity about pH 5.5 the second carboxyl group would be completely in the anion form and so the complex exists as the chelate. Above pH 5.5 a decrease of decarboxylation is observed but there is also a simultaneous increase in the absorption (cf. Figure 7). The absorbing species of the magnesium-oxalacetate complex involves the conjugated bonds of the enol form of the complex. This is evidence that it is the lower absorbing keto form of the complex that is the active species in decarboxylation:

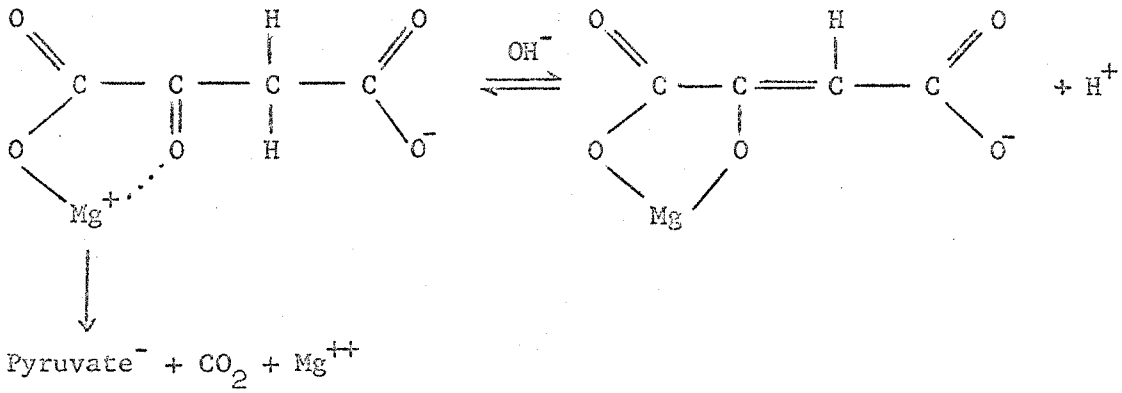

$$\text{Pyruvate}^- + CO_2 + Mg^{++}$$

At pH 7.4 there is a convergence of activity (isokinetic point) such that the rate constant is independent of magnesium ion concentration above a certain critical concentration. Above pH 7.4 increases in the concentration of magnesium ion decrease the rate of decarboxylation. This behaviour can be explained by the following equilibrium:

Active Keto

Inactive Enol

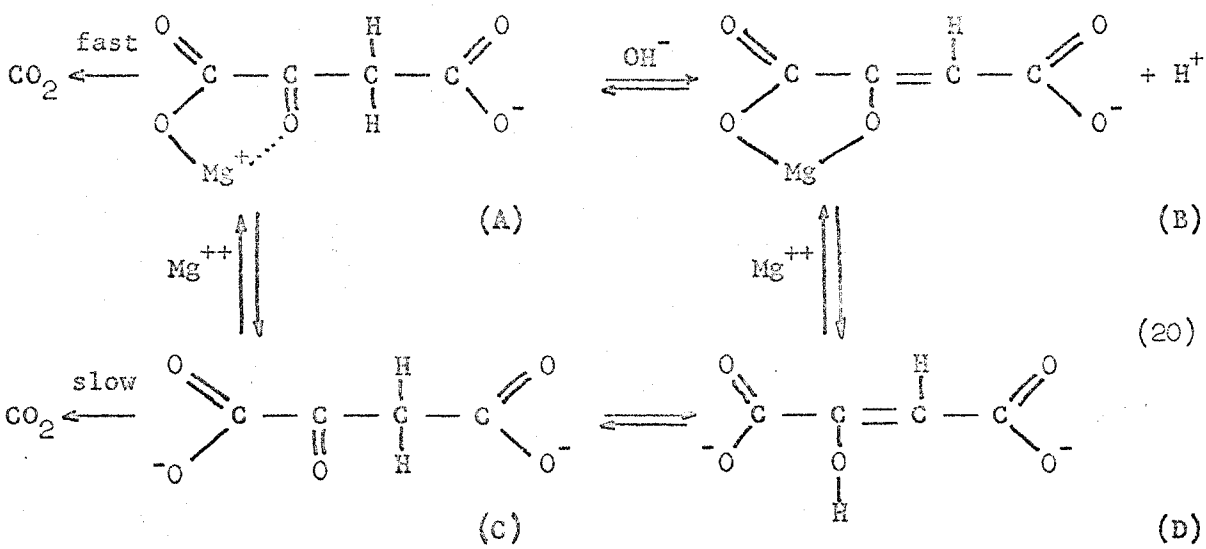

This equilibrium system can be considered under various conditions that displace the position of the equilibrium (indicated by heavy arrows) and so change the concentration of the active species (A).

i) With high concentration of magnesium ion at pH 5.5 the rate is the fastest:

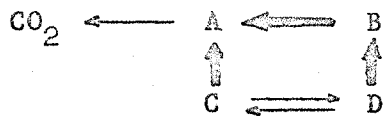

(21)

At pH values below 7.4 increases in the concentration of magnesium ion increase the rate of the decarboxylation until the 1:1 complex (A) is formed.

ii) With high concentration of magnesium ion at pH 8 the reaction is slower since the (B) form of the complex is favored:

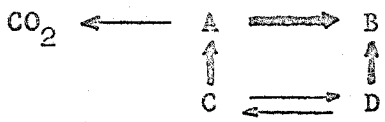

(22)

And so at pH values above pH 7.4 increases in magnesium chloride concentration above 0.1 M decrease the rate of decarboxylation. Further, the charge on the carboxylate ion needed for decarboxylation may be hindered by high magnesium ion concentration.

iii) With intermediate concentrations of magnesium ion at pH 8 decarboxylation is faster than in case ii):

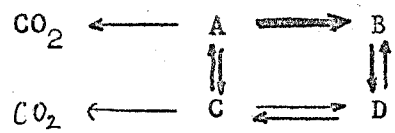

(23)

Under conditions of intermediate magnesium ion concentration the (B) form of the complex is not as favored and can decarboxylate by cycling through forms (D) and (C).

iv) At the isokinetic point of pH 7.4 the formation of the 1:1 complex takes place at lower magnesium ion concentrations than at pH 5 to 6. Further increases of magnesium ion have no effect on the saturated intermediate (A) and the observed rate constant is independent of the magnesium ion concentration.

v) At low concentrations of magnesium ion the rate of reaction is slow and almost independent of pH.

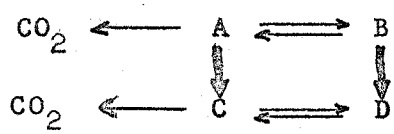

(24)

The effective magnesium ion concentration is either too low to form the 1:1 complex or too low to bind all the oxalacetate.

In D_2O the shift of the isokinetic point (Figure 6b) to pD 7.8

is evidence of the increased strength of the C–D bond in the enolization of the magnesium-oxalacetate complex. The spectrophotometric titration curve (Figure 7) gives further evidence of the shift of the equilibrium position between the keto and enol forms of the complex. The isotope rate effect k_{H_2O}/k_{D_2O} of 1.1 (ratio of first order rate constants at the isokinetic point) is indicative of a secondary isotope rate effect due to the deuterated keto form of the complex in which the two alpha hydrogens are replaced by deuterium.

It has been proposed (14) that the decrease in absorption observed when oxalacetate decarboxylates in the presence of metal ion is due to the ketonization of the enol-pyruvate complex which is the first product of decarboxylation. This interpretation was based on the assumption that the enol-pyruvate complex is a very strongly absorbing species compared to the oxalacetate-complex, but no spectral evidence was presented for this assumption. The present calculations for the absorbancy index of the keto and enol magnesium complexes, which combine kinetic and spectral data, account for all the predominate absorptions changes in the reaction without assuming a highly absorbing enol-pyruvate complex intermediate. The fast increase of absorption on the addition of magnesium ion to oxalacetate (Figure 9) is interpreted as the fast formation of the more strongly absorbing magnesium-oxalacetate complex. This fast formation was also observed for Al^{+++} (10), Cu^{++} and Zn^{++} (14). The decrease of absorption during decarboxylation can be accounted for by the decrease in the concentration of the absorbing magnesium-oxalacetate complex under various conditions of pH and magnesium ion concentration.

The absorption of the enol form predominates ($a_{enol} = 8.05 \times 10^3$, $a_{keto} = 5.38 \times 10^2$). And further, no primary isotope rate effect is observed as might be expected in the initial hydrolysis of the magnesium-enol-pyruvate complex during ketonization in D_2O.

The magnesium-ion-catalyzed decarboxylation is analogous to the behavior of other metals; in its pH dependence to copper (8,18,19), and in its inhibition effect at higher concentrations to Pb^{++}, Cu^{++}, La^{++}(5, 14).

Comparison of the effect of pH and pD on the rate of the magnesium-ion-catalyzed decarboxylation and the effect of pH and pD on the decarboxylation reaction catalyzed by oxalacetate carboxylase of Micrococcus lysodeikticus (35, 36) shows that both systems have the same maximum of activity at about pH 5.5 and that both peaks are shifted to higher pD values in the D_2O systems (35). Other enzymes that decarboxylate oxalacetic acid also have certain common features in their mechanism. The malic enzyme (37) from pigeon liver which depends on manganese ion or magnesium ion has a maximal activity at pH 4.5 to 5.0 and the enzyme from wheat germ has a maximal activity at pH 5.2. The oxalacetate carboxylase of chicken liver (38) which depends on inosine triphosphate has a maximal activity at about pH 6.0. The oxalacetate decarboxylase of rat liver (45) with a maximal activity at pH 7.4 depends on magnesium ion and is inhibited by manganese ion. The inhibition of the magnesium-ion-catalyzed decarboxylation of oxalacetate at high concentration of magnesium ion above pH 7.4 is analogous to the behavior of phosphoenol pyruvate carboxylase (46) from spinach leaves in the formation of oxalacetate where at 7.4 the reaction is stimulated by magnesium ion concentrations up to 2×10^{-3} M magnesium chloride and inhibited above this concentration.

IV. SUMMARY

Studies of the spontaneous decarboxylation of oxalacetic acid in Tris-acetate buffer systems in H_2O and D_2O over a range of pH and pD confirm that the cyclic mono-anion intermediate is the predominant active species that decarboxylates. The magnesium-ion-catalyzed decarboxylation follows a bell-shaped activity curve with a maximum rate between pH(pD) 5-6, indicating that the keto form of the magnesium-oxalacetate complex is the kinetically active species in decarboxylation. Spectrophotometric investigations show the presence of the enol form of the chelate which does not decarboxylate. A convergence of activities occurs at pH 7.4 (isokinetic point) which represents a point where the average activity of the keto form of the complex falls to half of its maximal value. The corresponding pH (or pD) value is the pK for the keto-enol chelate equilibrium. The ratio of the observed first order rate constants at the isokinetic point of $k_{H_2O}/k_{D_2O} = 1.1$ indicates a secondary isotope rate effect. The absorbancy index of the keto and enol forms of the chelate as well as the keto-enol equilibria of the magnesium-oxalacetate complex at various pH(pD) values were calculated from a combination of kinetic and spectral data. The absorption changes observed during decarboxylation are accounted for in terms of concentration changes of the keto and enol forms of the magnesium-oxalacetate complex without assuming that the intermediate enol-pyruvate complex is strongly absorbing. The behavior of the magnesium-ion-catalyzed system furthers the parallelisms between the mechanism of the metal ion and enzymatic decarboxylation of oxalacetic acid.

REFERENCES

(1) H. A. Krebs, Biochem. J., 36, 303, (1942).

(2) S. Ochoa, J. Biol. Chem., 174, 115, (1948).

(3) F. Lynen and H. Scherer, Ann., 560, 163, (1948).

(4) P. Ostern, Ztschr. fur Physiol. Chem. 218, 160, (1933).

(5) J. F. Speck, J. Biol. Chem., 178, 315, (1949).

(6) P. Nossal, Austr. J. Exptl. Biol. Med. Sci., 27, 143, (1949).

(7) P. Nossal, ibid. 27, 312, (1949).

(8) P. Nossal, Nature, 163, 405, (1949).

(9) K. J. Pedersen, Acta. Chem. Scand., 6, 285, (1952).

(10) A. Kornberg, S. Ochoa and A. Mehler, J. Biol. Chem., 174, 159, (1948).

(11) E. Gelles, J. Chem. Soc., 4736, (1956).

(12) E. Gelles, J. Inorg. and Nuclear Chem., 8, 625, (1958).

(13) E. Gelles, and J. Clyton, Trans. Farad. Soc., 52, 353, (1956).

(14) E. Gelles and R. W. Hay, Part I. J. Chem. Soc., 3673, (1958).

(15) E. Gelles and A. Salama, Part II. ibid 3683, (1958).

(16) E. Gelles and A. Salama, Part III. ibid 3689, (1958).

(17) L. O. Krampitz and C. H. Werckman, Biochem. J., 35, 595, (1941).

(18) R. Steinberger and F. H. Westheimer, J. Am. Chem.,Soc., 71, 4158, (1949).

(19) R. Steinberger and F. H. Westheimer, J. Am. Chem. Soc., 73, 429, (1951).

(20) B. Brown, Quat. Reviews, 5, 131, (1951).

(21) K. Widmark, Acta. Med. Scand., 53, 393, (1920).

(22) K. J. Pedersen, J. Am. Chem. Soc., 51, 2098, (1929).

(23) Bredis and Balcom, Ber. 41, 740, (1908).

(24) Franke and Brathuhm, Ann. 487, 1, (1931).

(25) E. Wiig, J. Phys. Chem., 32, 961, (1928).

(26) G. Hall, J. Am. Chem. Soc., 71, 2691, (1949).

(27) E. Gelles, J. Am. Chem. Soc., 75, 6199, (1953).

(28) R. Davies, Biochem. J., 37, 230, (1943).

(29) E. A. Evans, J. Biol. Chem. 35, 595, (1943).

(30) G. W. E. Plant and H. Lardy, J. Biol. Chem., 180, 13, (1949).

(31) V. Salles, I. Harary, R. Banti and S. Ochoa, Nature, 165, 675, (1950).

(32) V. Salles and S. Ochoa, J. Biol. Chem., 187, 849, (1950).

(33) S. K. Alice del Comillo and S. Ochoa, J. Biol. Chem., 187, 891, (1950).

(34) F. H. Westheimer, Transac. N. Y. Acad. of Sci., 18, 15, (1955).

(35) S. Seltzer, G. A. Hamilton and F. H. Westheimer, J. Am. Chem. Soc., 81, 4018, (1959).

(36) D. Herbert, Symposia Soc. Exptl. Biol., 4, 52, (1951).

(37) S. Ochoa, In Methods in Enzymology Vol. I, S. P. Colowick and N. O. Kaplan (Editors), Acad. Press Inc. N. Y., 1955, p. 739.

(38) M. F. Utter, K. Kurahashi and I. A. Rose, J. Biol. Chem., 207, 803, (1954).

(39) R. Lumry, E. L. Smith and R. R. Glantz, J. Am. Chem. Soc., 73, 4330, (1951).

(40) R. L. Scott, Rec. Trav. de Chim., 75, 787, (1956).

(41) H. A. Benesi and J. Hildebrand, J. Am. Chem. Soc., 71, 2703, (1949).

(42) G. W. Kosicki, Canad. J. Chem., 40, 1280, (1962).

(43) K. J. Pedersen, Acta. Chem. Scand., 6, 243, (1952).

(44) N. Li, Ph. Tang, and R. Mathur, J. Phys. Chem., 65, 1074, (1961).

(45) L. M. Corwin, J. Biol. Chem., 234, 1338, (1959).

(46) R. S. Bandurski and F. Lipman, J. Biol. Chem., 219, 741, (1956).

APPENDIX I

An example of kinetic data used in Fig. 5 a, b. They are the set of measurements made at 25.0°C., 0.5 cm light path and pH=8 with varying magnesium ion concentration.

$[MgCl_2]$ = 0.96M A_e = 0.055 k graph = 0.0052 min^{-1}

A_o = 0.585 λ = 278mμ k aver. = 0.0054 min^{-1}

t (min)	A_t	$\frac{2.303}{t}$	$\log\frac{A_o - A_e}{A_t - A_e}$	k(min^{-1})
3.0	0.574	0.7676	0.0091	0.0069
8.5	0.555	0.2709	0.0253	0.0068
10.0	0.550	0.2303	0.0296	0.0068
12.5	0.547	0.1842	0.0305	0.0056
18.5	0.530	0.1244	0.0475	0.0059
27.5	0.510	0.0837	0.0662	0.0055
31.5	0.500	0.0731	0.0759	0.0055
58.0	0.449	0.0397	0.1287	0.0051
62.0	0.438	0.0371	0.1410	0.0052
65.0	0.434	0.0354	0.1456	0.0051
78.0	0.409	0.0295	0.1752	0.0051
88.0	0.390	0.0261	0.1985	0.0051
105.5	0.360	0.0218	0.2399	0.0052
126.0	0.325	0.0182	0.2929	0.0053
153.5	0.286	0.0150	0.3606	0.0054
193.0	0.239	0.0119	0.4594	0.0054
∞	0.055			

Fig. 10 (e); Fig. 11 (1)

$[MgCl_2]$ = 0.64 M A_e = 0.020 k graph = 0.0092 min^{-1}

A_o = 0.720 λ = 278 mμ k aver. = 0.0093 min^{-1}

t (min)	A_t	$\frac{2.303}{t}$	$\log \frac{A_o - A_e}{A_t - A_e}$	K(min^{-1})
2.5	0.699	0.9212	0.0132	0.0121
4.0	0.690	0.5757	0.0190	0.0109
5.0	0.681	0.4606	0.0249	0.0114
8.0	0.669	0.2878	0.0328	0.0094
14.5	0.631	0.1588	0.0590	0.0093
23.0	0.588	0.1001	0.0907	0.0090
24.0	0.582	0.0959	0.9536	0.0091
32.5	0.548	0.0708	0.0122	0.0086
39.0	0.514	0.0590	0.1513	0.0089
43.0	0.491	0.0535	0.1720	0.0092
55.0	0.445	0.0418	0.2167	0.0090
75.0	0.370	0.0307	0.3010	0.0092
94.0	0.315	0.0245	0.3752	0.0091
110.5	0.272	0.0208	0.4437	0.0092
129.0	0.230	0.0178	0.5228	0.0093
148.0	0.195	0.0155	0.6020	0.0093
164.0	0.170	0.0140	0.6690	0.0093
193.0	0.131	0.0119	0.7997	0.0095
248.0	0.082	0.0092	1.0527	0.0097
265.0	0.071	0.0086	1.1393	0.0099
285.0	0.060		1.2430	
295.0	0.055			
315.0	0.045			
380.0	0.020			

Fig. 10 (-); Fig. 11 (2).

$[MgCl_2]$ = 0.026 M A_o = 0.370 k graph = 0.0139 min^{-1}

λ = 278 mμ A_e = 0.030 k aver. = 0.0136 min^{-1}

t (min)	A_t	$\frac{2.303}{t}$	$\log \frac{A_o - A_e}{A_t - A_e}$	k(min^{-1})
5.0	0.384	0.4606	0.0290	0.0133
6.5	0.340	0.3543	0.0401	0.0142
8.0	0.336	0.2878	0.0457	0.0131
9.5	0.330	0.2424	0.0543	0.0131
11.0	0.324	0.2093	0.0631	0.0132
12.5	0.319	0.1842	0.0705	0.0130
14.0	0.313	0.1645	0.0796	0.0131
15.5	0.305	0.1485	0.0921	0.0136
17.0	0.301	0.1354	0.0985	0.0133
18.5	0.296	0.1244	0.1115	0.0138
20.0	0.290	0.1151	0.1165	0.0134
23.5	0.281	0.0980	0.1318	0.0129
27.0	0.268	0.0852	0.1549	0.0132
30.5	0.256	0.0755	0.1773	0.0133
34.5	0.241	0.0667	0.2061	0.0137
39.0	0.230	0.0590	0.2293	0.0135
44.0	0.217	0.0523	0.2596	0.0135
45.5	0.212	0.0506	0.2702	0.0136
47.0	0.209	0.0490	0.2786	0.0136
57.0	0.185	0.0404	0.3397	0.0137
58.5	0.182	0.0393	0.3496	0.0137
64.0	0.171	0.0359	0.3822	0.0137
69.0	0.160	0.0333	0.4175	0.0139
73.0	0.154	0.0315	0.4380	0.0138
78.0	0.143	0.0295	0.4780	0.0141
83.5	0.134	0.0275	0.5123	0.0141
88.5	0.129	0.0260	0.5358	0.0139
95.0	0.119	0.0242	0.5796	0.0140
102.0	0.111	0.0225	0.6203	0.0140
109.0	0.101	0.0211	0.6802	
116.0	0.095	0.0198	0.7185	
124.0	0.086	0.0185	0.7832	
133.0	0.079	0.0173	0.8412	
196.0	0.044			
	0.030			

Fig. 10 (c); Fig. 11 (3).

$[MgCl_2]$ = 0.040 M A_o = 0.960 k graph = 0.0176 min^{-1}

λ = 278 mμ A_e = 0.040 k aver. = 0.0170 min^{-1}

t (min)	A_t	$\frac{2.303}{t}$	$\log \frac{A_o - A_e}{A_t - A_e}$	k(min^{-1})
5.5	0.884	0.4187	0.0374	0.0156
7.0	0.865	0.3290	0.0473	0.0155
8.5	0.843	0.2709	0.0590	0.0160
10.0	0.823	0.2303	0.0700	0.0161
11.5	0.802	0.2093	0.0818	0.0171
13.0	0.783	0.1771	0.0928	0.0164
14.5	0.763	0.1588	0.1046	0.0166
16.0	0.743	0.1439	0.1168	0.0168
17.5	0.723	0.1316	0.1290	0.0169
19.0	0.706	0.1212	0.1403	0.0170
20.5	0.688	0.1123	0.1522	0.0170
24.0	0.648	0.0959	0.1798	0.0172
27.5	0.613	0.0837	0.2056	0.0172
31.0	0.578	0.0742	0.2330	0.0173
35.0	0.541	0.0658	0.2639	0.0173
39.5	0.505	0.0583	0.2963	0.0172
44.5	0.476	0.0517	0.3243	0.0167
46.0	0.457	0.0500	0.3436	0.0172
47.5	0.446	0.0484	0.3552	0.0172
52.5	0.413	0.0438	0.3920	0.0171
57.5	0.384	0.0400	0.4272	0.0171
59.0	0.374	0.0390	0.4393	0.0171
64.5	0.345	0.0347	0.4787	0.0170
69.5	0.320	0.0331	0.5166	0.0171
73.5	0.300	0.0313	0.5488	0.0171
78.5	0.277	0.0293	0.5890	0.0172
84.0	0.254	0.0274	0.6333	0.0173
89.0	0.235	0.0258	0.6726	0.0174
95.5	0.212	0.0241	0.7282	0.0175
102.5	0.191	0.0224	0.7833	0.0176
109.5	0.172	0.0210	0.8432	0.0177
116.5	0.156	0.0197	0.8993	0.0177
124.5	0.138	0.0184	0.9703	0.0179
133.5	0.123			
196.5	0.057			
∞	0.040			

Fig. 10 (f); Fig. 11 (4).

$[MgCl_2]$ = 0.05 M A_o = 0.800 k graph = 0.0216 min^{-1}

λ = 278 mμ A_e = 0.025 k aver. = 0.0217 min^{-1}

t (min)	A_t	$\frac{2.303}{t}$	$\log \frac{A_o - A_e}{A_t - A_e}$	k(min^{-1})
6.0	0.699	0.3838	0.0606	0.0232
7.5	0.677	0.3070	0.0750	0.0230
9.0	0.657	0.2558	0.0885	0.0226
10.5	0.637	0.2193	0.1025	0.0224
12.0	0.618	0.1919	0.1158	0.0222
13.5	0.599	0.1705	0.1300	0.0221
15.0	0.582	0.1535	0.1434	0.0220
16.5	0.564	0.1395	0.1573	0.0219
18.0	0.548	0.1279	0.1709	0.0218
19.5	0.532	0.1181	0.1842	0.0217
21.0	0.517	0.1096	0.1973	0.0216
24.5	0.483	0.0940	0.2284	0.0214
28.0	0.451	0.0822	0.2598	0.0213
31.5	0.419	0.0731	0.2932	0.0214
35.5	0.390	0.0648	0.3270	0.0212
40.0	0.358	0.0575	0.3668	0.0211
45.0	0.327	0.0511	0.4092	0.0209
46.5	0.318	0.0495	0.4224	0.0209
48.0	0.309	0.0479	0.4359	0.0209
53.0	0.278	0.0434	0.4853	0.0210
58.0	0.252	0.0397	0.5332	0.0211
59.5	0.245	0.0387	0.5468	0.0211
65.0	0.219	0.0354	0.6003	0.0212
70.0	0.199	0.0329	0.6487	0.0213
74.0	0.183	0.0311	0.6906	0.0214
79.0	0.166	0.0291	0.7400	0.0215
84.5	0.148	0.0272	0.7976	0.0217
89.5	0.136	0.0257	0.8439	0.0217
96.0	0.119	0.0239	0.9138	0.0219
103.0	0.105	0.0223	0.9862	0.0220
110.0	0.092	0.0209	1.0632	
118.0	0.082		1.1334	
125.0	0.070		1.2312	
134.0	0.060		1.3390	
197.0	0.025			

Fig. 10 (d); Fig. 11 (5).

$[MgCl_2]$ = 0.128 M A_o = 0.222 K graph = 0.0288 min^{-1}

λ = 278 mμ A_e = 0.002 k aver. = 0.0286 min^{-1}

t (min)	A_t	$\frac{2.303}{t}$	$\log \frac{A_o - A_e}{A_t - A_e}$	k(min^{-1})
3.5	0.204	0.6580	0.0370	0.0243
5.5	0.188	0.4187	0.0729	0.0305
9.0	0.171	0.2558	0.1145	0.0293
10.5	0.165	0.2193	0.1302	0.0285
13.0	0.155	0.1771	0.1577	0.0279
18.5	0.131	0.1244	0.2318	0.0288
27.5	0.102	0.0837	0.3424	0.0286
58.5	0.045	0.0393	0.7089	0.0279
62.5	0.039	0.0368	0.7683	0.0283
66.0	0.036	0.0348	0.8109	0.0282
78.5	0.025	0.0293	0.9806	0.0287
88.5	0.020	0.0260	1.0871	0.0282
106.0	0.013	0.0217	1.3010	0.0282
126.5	0.007	0.0182	1.6020	0.0291
154.5	0.005	0.0149	1.8653	0.0278
194.0	0.002			

Fig. 10 (a); Fig. 11 (6).

$[MgCl_2]$ = 0.09 M A_o = 0.325 k graph = 0.0301 min^{-1}

λ = 278 mμ A_e = 0.002 k aver. = 0.0297 min^{-1}

t (min)	A_t	$\frac{2.303}{t}$	$\log \frac{A_o - A_e}{A_t - A_e}$	k(min^{-1})
2.5	0.307	0.9212	0.0249	0.0229
4.5	0.284	0.5117	0.0589	0.0301
7.0	0.269	0.3290	0.0826	0.0272
8.0	0.256	0.2878	0.1043	0.0300
9.5	0.245	0.2424	0.1235	0.0299
12.0	0.230	0.1919	0.1512	0.0290
18.0	0.191	0.1279	0.2327	0.0297
27.0	0.146	0.0852	0.3508	0.0299
31.0	0.130	0.0742	0.4019	0.0298
57.5	0.060	0.0400	0.7457	0.0298
61.0	0.055	0.0377	0.7849	0.0296
64.5	0.049	0.0357	0.8371	0.0298
77.5	0.034	0.0297	1.0040	0.0298
87.5	0.025	0.0264	1.1474	0.0303
105.0	0.015	0.0219	1.3952	0.0305
125.5	0.009			
153.0	0.004			
192.0	0.002			

Fig. 10 (b); Fig. 11 (7).

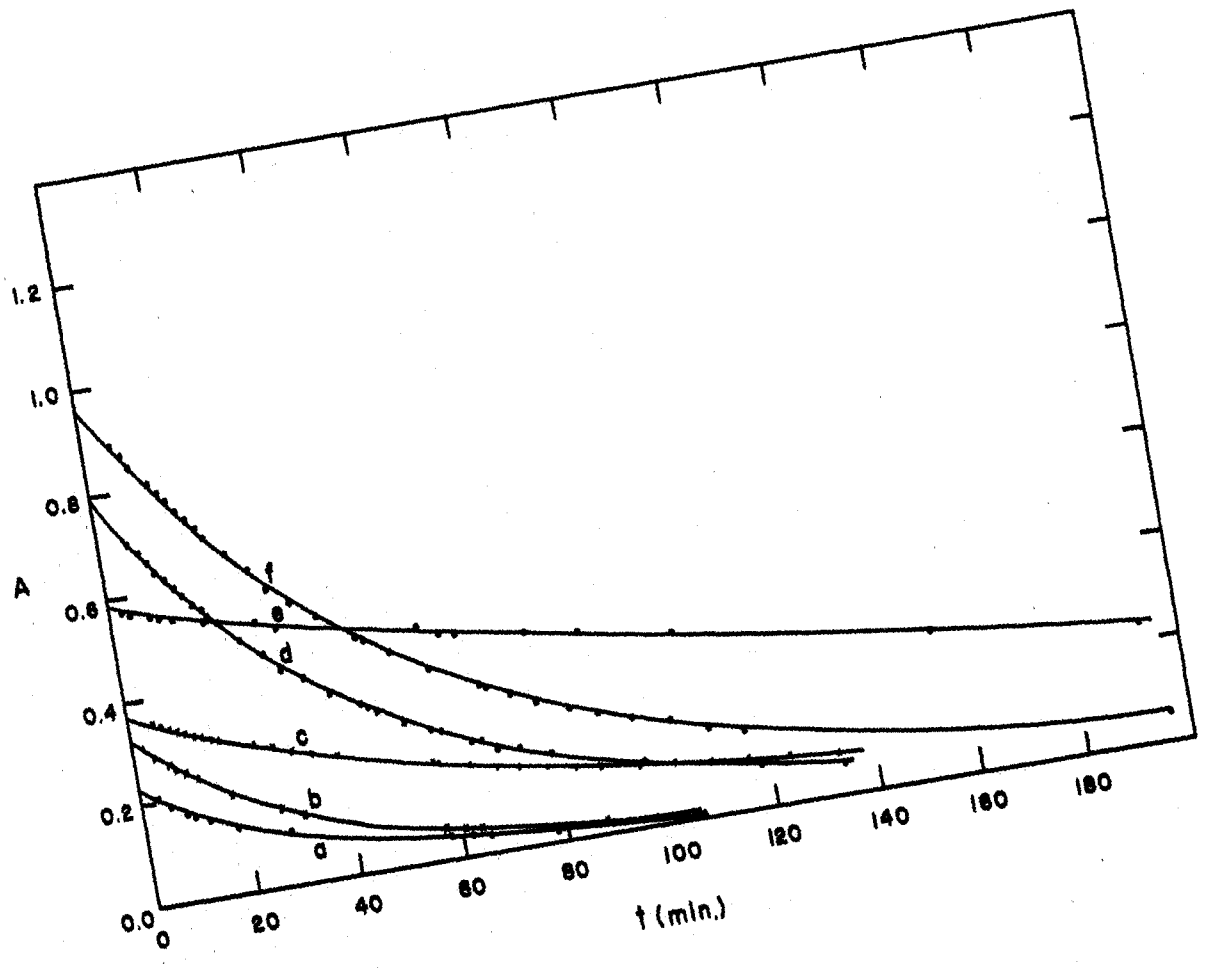

Fig. 10.

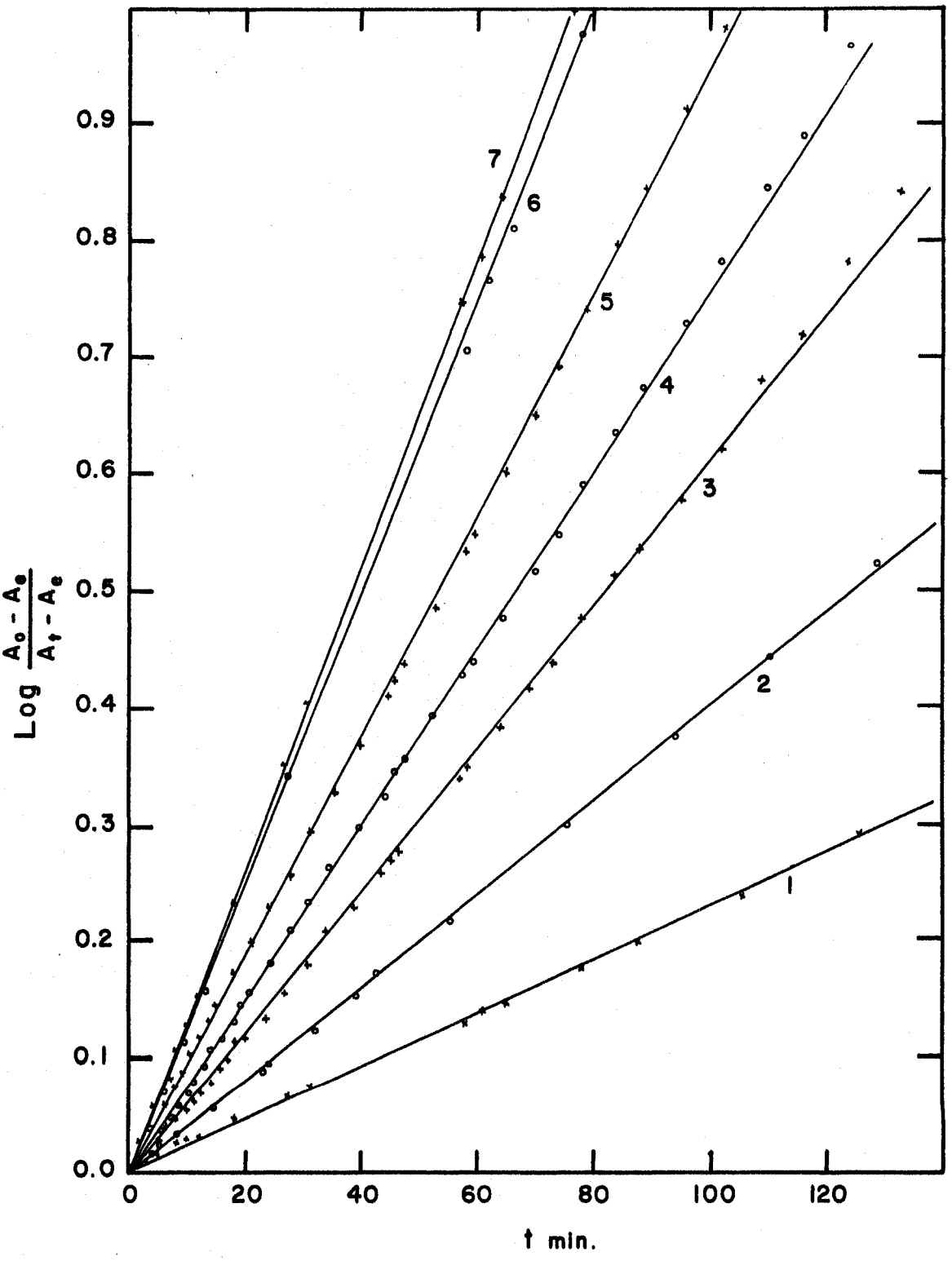

Fig. 11.

Figures 10 and 11

Legend: Each cuvette (0.5 cm light path) contained 0.3 - 0.5 M Tris-acetate buffer pH = 8, $\sim$ 2X 10^{-4} M oxalacetic acid and varying concentration of $MgCl_2$.

Fig. 11 Signature of the straight line	Fig. 10 Signature of the curve	$MgCl_2$ mols.	Table page
1	e	0.96	51
2	-	0.64	52
3	c	0.026	53
4	f	0.040	54
5	d	0.05	55
6	a	0.128	56
7	b	0.09	57

APPENDIX II

Details of the calculation of the absorbancy index of the keto form of magnesium-oxalacetate complex in Tris-acetate buffer at pH $\geqslant$ 5.5, 1 cm light path, making the assumption as listed on pages 28 and 29.

C_T - total concentration of the complex.

C_E - concentration of the enol form of the complex

C_K - concentration of the keto form of the complex

A_T - total absorbance at 280 mμ (pH = 5.5)

a_E - absorbancy index of the enol form of Mg-OAA complex (at 280 mμ)

a_K - absorbancy index of the keto form of Mg-OAA complex (at 280 mμ)

The prime numbers refer to the values at one half of the maximal activity (pH = 7.4).

$$S = C_T = C_E + C_K = C'_T = C'_E + C'_K$$

$$Q = A_T = a_E C_E + a_K C_K$$

$$R = A'_T = a_E C'_E + a_K C'_E$$

$$M = a_E$$

$$C'_K = \frac{C_K}{2}; \quad C_K = C_T - C_E ; \quad C_K = C_T - C'_E + \frac{C_K}{2}$$

$$Q = MC_E + a_K C_K$$

$$R = MC'_E + a_K C'_K = M\left[C_E + \frac{C_K}{2}\right] + a_K \frac{C_K}{2}$$

$$Q = MC_E + a_K C_K$$

$$R = MC_E + (M + a_K)\frac{C_K}{2}\Big/ 2$$

$$Q = MC_E + a_K C_K$$

$$2R = 2MC_E + (M + a_K)C_K$$

$$C_K = \frac{\begin{vmatrix} M & Q \\ 2M & 2R \end{vmatrix}}{\begin{vmatrix} M & a_K \\ 2M & M + a_K \end{vmatrix}}$$

$$C_K = \frac{2MR - 2MQ}{M(M + a_K) - 2Ma_K} = \frac{2R - 2Q}{M - a_K}$$

$$C_E = \frac{\begin{vmatrix} Q & a_K \\ 2R & M + a_K \end{vmatrix}}{\begin{vmatrix} M & a_K \\ 2M & M + a_K \end{vmatrix}}$$

$$C_E = \frac{Q(M + a_K) - 2Ra_K}{M(M + a_K) - 2Ma_K} = \frac{Q(M + a_K) - 2Ra_K}{M(M - a_K)}$$

$$S = C_E + C_K ; \quad S - C_E = C_K$$

$$S - \frac{Q(M + a_K) - 2Ra_K}{M(M - a_K)} = \frac{2R - 2Q}{M - a_K}$$

$$SM^2 - SMa_K - QM - Qa_K - 2Ra_K = 2RM - 2QM$$

$$M(SM - Q - 2R + 2Q) = a_K(SM + Q + 2R)$$

$$a_K = \frac{M(SM + Q - 2R)}{SM + Q + 2R}$$

$$a_K = \frac{a_E\left(A_T + C_T a_E - 2A'_T\right)}{A_T + C_T a_E + 2A'_T}$$

VITA

The author was born in Titograd, Yugoslavia, on December 24, 1933, the fifth of six children of Jelena and Nikola Dragovic.

In 1952 the author enrolled at the Faculty of Natural Sciences and Mathematics, University of Belgrad, from which she received a Faculty Diploma in February, 1957. After graduation, the author was appointed as an University Assistant in the Department of Physical Chemistry, University of Belgrad.

The following papers have been published since that time:

S. Ristic and S. Lipovac: Spectrophotometric Measurements on Natural and Irradiated Kunzite. Bull. of the Inst. of Nuclear Sci. 'Boris Kidrich' 9, 77 (1959).

J. Nedeljkovic, S. Ristic and S. Lipovac: Spectres d' adsorption du 'Biofil' et quelques tuberkulines. 'Recuel des articles sur le Biofil', p. 163, Belgrad, 1960.

S. Lipovac: Specrophotometric Investigation of 3,4 Benzpyrene in several organic solvents, Documenta Chemica Yugoslavica. Bull. de la Soc. Chim. Belgrad, 25-26, 81, (1961).

S. Lipovac and M. Stefanovic: Coulometric Method for the Determination of Molar Ratio of Inclusion Compounds of Deoxycholic Acid. Glas de l'Academie Serbe des Science et des Arts CCLIII, Class des Sciences mathématiques et naturelles No. 23, p.105, (1963).